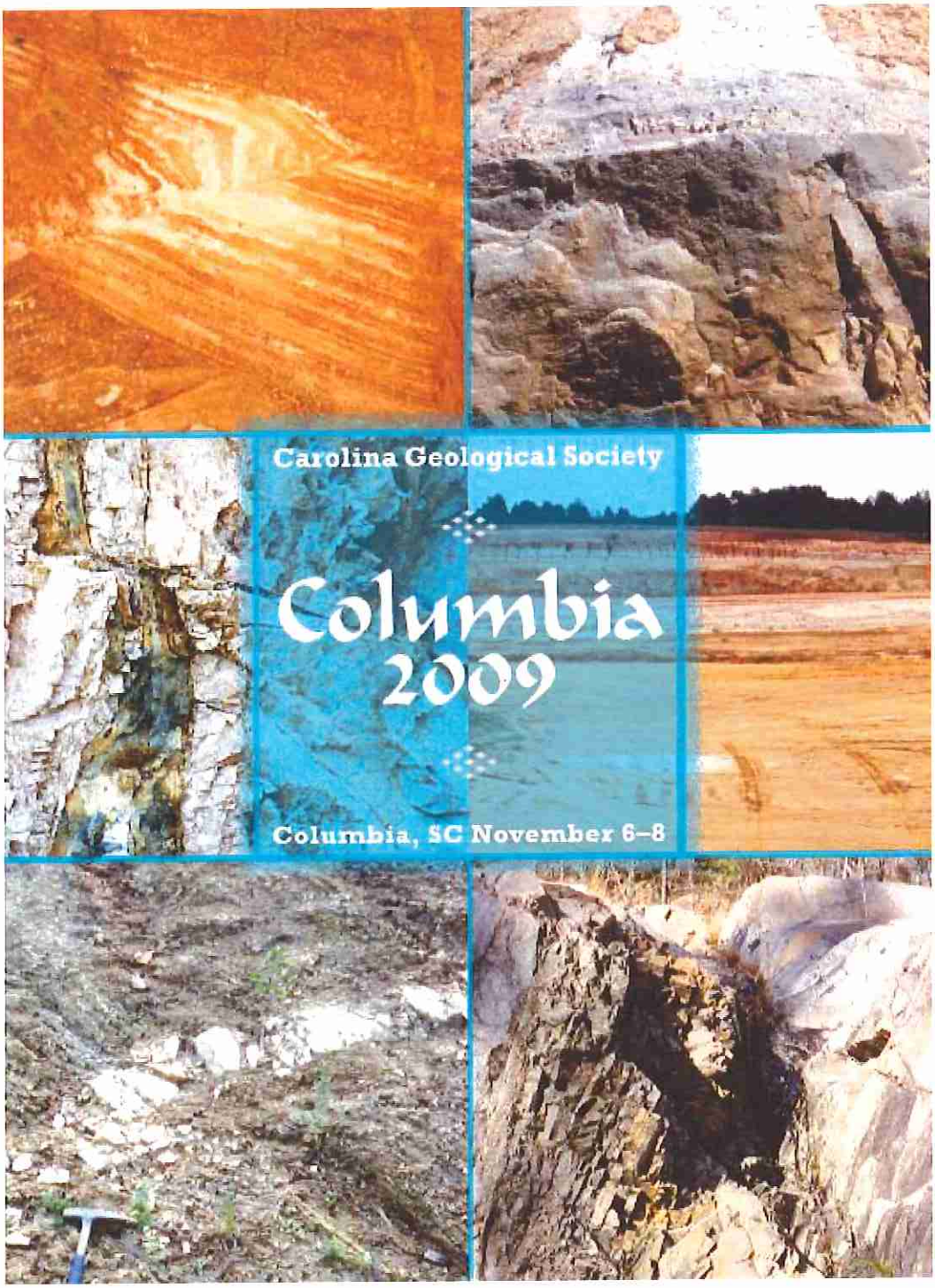
Carolina Geological Society
Columbia
2009
Columbia, SC November 6–8

Fieldtrip — Annual Meeting Carolina Geological Society

Georgia Southern University Department of Geology and Geography Contribution Series, No. 2

Clarion Hotel — Columbia, SC
6 - 8 November 2009

Local Committee for the Fieldtrip

Mervin J. Bartholomew, Department of Earth Sciences, University of Memphis, Memphis, TN

Mark A. Evans, Department of Physics and Earth Sciences, Central Connecticut State University, New Britain, CT

Fredrick J. Rich, Department of Geology and Geography, Georgia Southern University, Statesboro, GA

Brendan M Brodie, Earth Con, Inc., Greenville, SC

R. Daniel Heath, Sammamish, WA

Fieldguide layout – M.J. Bartholomew and Hans Mortensen

RIFTING AND DRIFTING IN SOUTH CAROLINA: FRACTURE HISTORY IN ALLEGHANIAN GRANITES AND COASTAL PLAIN STRATA

Mervin J. Bartholomew, *Department of Earth Sciences, University of Memphis, Memphis, TN 38152*

Mark A. Evans, *Department of Physics and Earth Sciences, Central Connecticut State University, New Britain, CT 06050*

Fredrick J. Rich, *Department of Geology and Geography, Georgia Southern University, Statesboro, GA 30460*

Brendan M. Brodie, *Earth Con, Inc., 3440 Augusta Road, Greenville, SC 29605*

R. Danial Heath, *1515 212th Avenue NE, Sammamish, WA 98074*

INTRODUCTION

We have used a series of field trips (Bartholomew *et al.*, 1994, 1998, 2000, 2007; Wooten *et al.*, 2001) and publications (Bartholomew *et al.*, 2002; Bartholomew and Rich, 2007; Davis and Rich, 2005; Evans and Bartholomew, in press) to highlight some important localities in Alleghanian granites and older Piedmont gneisses (GA, SC, NC), in the Deep River Triassic basin (NC), and in Coastal Plain strata (GA, SC) where we have extensive fracture data for our ongoing analysis of the post-Alleghanian structural evolution of the southeastern part of the Laurentian craton (*Figure 1*). Most of the data were collected to understand when brittle fractures formed and their role in the larger geologic framework around the U.S. Department of Energy (USDOE) Savannah River Site near Aiken, SC, and the then-proposed low-level radioactive waste-disposal site in Wake County near Raleigh, NC. Subsequently, we expanded our studies to encompass late Quaternary fractures and features that provide insights into how the Atlantic passive margin deforms in the modern stress field (Bartholomew and Rich, 2001, 2002).

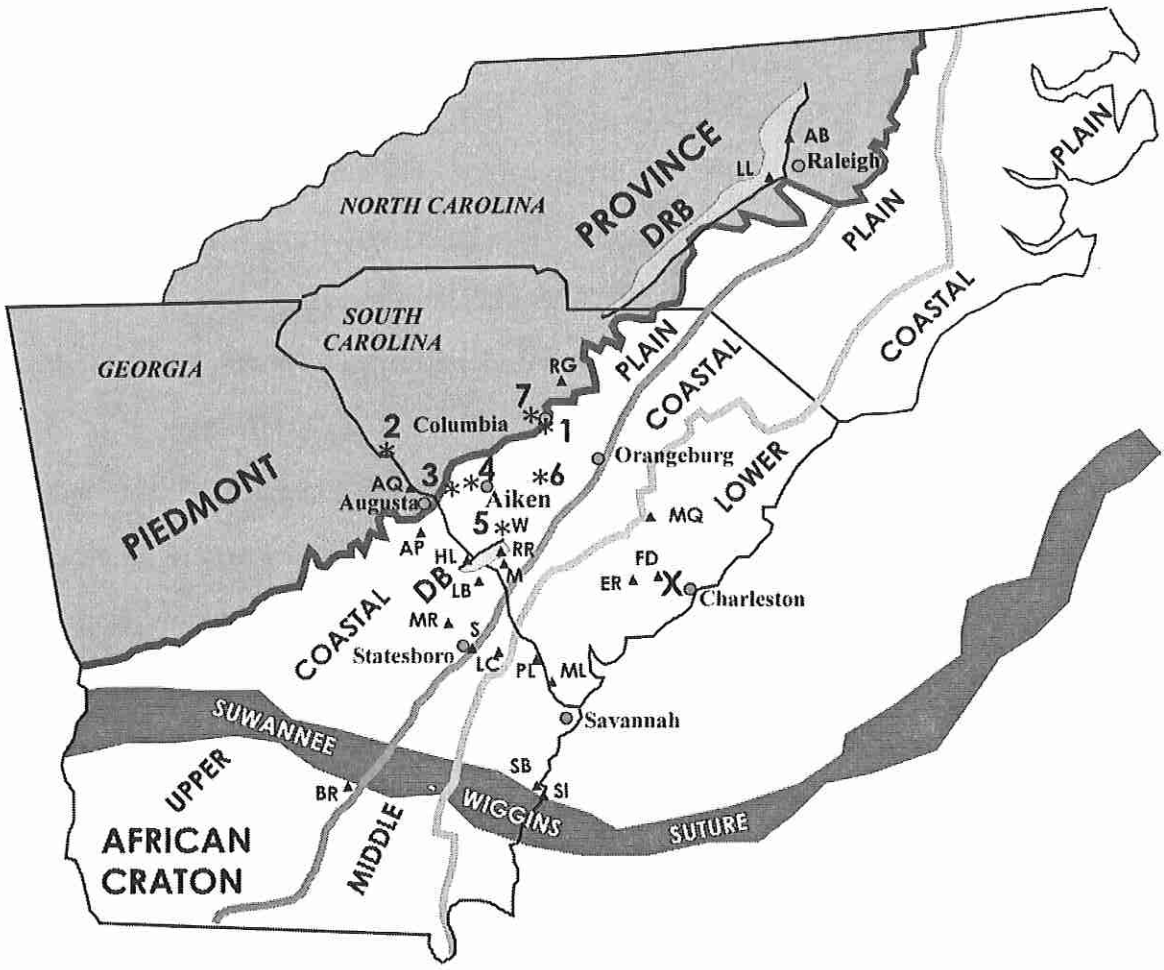

Figure 1. Location map showing field trip STOPS 1-7in South Carolina relative to: 1) the overlap of Coastal Plain strata over the crystalline Piedmont Province; 2) the African craton accreted during the Alleghanian orogeny along the Suwannee-Wiggins suture;3) the upper, middle, and lower divisions of the Atlantic Coastal Plain; and 4) localities described in our previous publications (Bartholomew et al., 2002; Bartholomew and Rich, 2007; Davis and Rich, 2005) and field trip guidebooks (Bartholomew et al., 1998, 2000, 2007; Wooten et al., 2001). Geology adapted from Bollinger (1977), Aadland et al. (1995), Colquhoun (1965, 1969); Colquhoun et al.(1983, 1987, 1991), Cumbest et al. (1992), Domoracki (1995), Dutton (1889), Fallaw and Price (1995), Hatcher et al. (2007), Hoyt and Hails (1974), Hoyt et al. (1968), Huddlestun (1988), Snipes et al. (1993a, b), Stieve and Stevenson (1995), Weems and Lewis (2002), and Willoughby et al. (1999). DB- subsurface Dunbarton Triassic Basin; DRB- Deep River Triassic Basin; X- epicenter for 1886 Charleston, SC earthquake. Localities: AB- Angus Barn; BR- Broxton Rocks; ER- Edisto River; FD- Fort Dorchester; HL- Hancock Landing;LL- potential low-level radioactive waste-disposal site; M- Martin; ML- Millstone Landing; MQ- Matin Marietta quarry; RG- Ridgeway gold mine; RR- Railroad cut on US DOE Savannah River Site; SB- Sutherland Bluff; SI- Sapelo Island; W- Williston. (Figure modified after Bartholomew et al., 2007).

Heath and Bartholomew (1997) suggested about nine regional structural events occurred during earlier phases of failed rifting during the Triassic and subsequent successful rifting related to the opening of the Atlantic Ocean and Jurassic. These events are represented by significant shifts in orientations and/or inversions of S_{Hmax} (maximum horizontal compressive stress), S_{Hmin} (minimum horizontal compressive stress), and S_v (vertical stress). Most of these Mesozoic events are accompanied by mineralization (e.g., pink staining or accumulation of chlorite, hematite, or calcite) and reflect changes in temperature and pressure as the Piedmont underwent uplift and exhumation (Evans and Bartholomew, in press). However, there are differences between the number of specific sequential Triassic events recognized at the Ridgeway Gold Mine (Bartholomew *et al.* (1998) versus at the Augusta Quarry (Bartholomew *et al.*, 2007) versus in and near the Deep River Basin (e.g., Wooten *et al.*, 2001) (Figure 1). Near the region of this field trip, the five events at the Ridgeway Gold Mine all correspond to specific events in the sequence at the Augusta Quarry where an additional four events are recognized. Thus we hope to eventually be able to define the geographic extent of both local and regional Triassic events. The same two Jurassic events are recognized at both of these localities as well as the initial Cretaceous event which is also recognized in overlying Cretaceous sediments (Brodie and Bartholomew, 1997).

Brodie and Bartholomew (1997) also suggested about nine events affected the Atlantic Coastal Plain strata since the onset of the drift phase and passive margin sedimentation during the Cretaceous. The earliest of these fracture sets, which is recognized only in Cretaceous sediments, coincides in orientation with the oldest, post-Jurassic, fracture set in crystalline rocks of the Piedmont recognized by Heath and Bartholomew (1997). Significant shifts in orientations of S_{Hmax}, S_{Hmin}, and S_v resulted in periods of surface deformation and erosion as well as changes in thickness in strata across faults (e.g., Prowell and O'Conner, 1978; Prowell, 1988; Bartholomew *et al.*, 2002).

Major events occurred during the Late Cretaceous (E-W- S_{Hmax}), Late Eocene (NE-SW-S_{Hmax}), Late Miocene (NNE-SSW-S_{Hmax}), and Late Quaternary (present-day; NE-SW-S_{Hmax}). The Eocene and Miocene multi-phase events are associated not only with easily recognizable reverse faults, but also with complex patterns of normal faults, joints, and some clastic dikes (e.g., Bartholomew et al., 2002, 2007). Moreover, because the orientation of S_{Hmax} during the Late Eocene was essentially the same as S_{Hmax} today, such features as the Late Eocene Williston growth-fault structure (Bartholomew *et al.*, 2002) serve as a model for predicting the orientation of major, seismically active NW-trending, SE-dipping basement fault-zones. Bartholomew and Rich (2007) analyzed fractures in the walls of colonial Fort Dorchester, which were produced by the 1886 Charleston earthquake (Dutton, 1889). They showed that these fracture sets in the walls were consistent with the present-day stress field as determined from the following: 1) regional Pleistocene/Holocene joint patterns of Bartholomew *et al.* (1998, 2000); 2) seismicity near Charleston, SC (e.g., Madabhushi and Talwani, 1993); and, 3) borehole breakouts in SC (Zoback *et al.*, 1978; Moos and Zoback, 1993). They used these orthogonal sets of both joints and conjugate normal faults to determine the likely orientation of the Dorchester fault that produced the 1886 Charleston earthquake. Their predicted orientation of this active fault zone was recently verified by better-located earthquake foci (Dura-Gomez and Talwani, 2009; Talwani and Dura-Gomez, 2009).

Most of the time from the Late Cretaceous to the Quaternary this region was characterized by extension ($S_v > S_{Hmax} > S_{Hmin}$), but *en echelon* joint arrays indicate that inversions of $\sigma 1$ and $\sigma 2$ ($S_{Hmax} > S_v > S_{Hmin}$) occurred, so that both $\sigma 1$ and $\sigma 3$ were horizontal. Thus fractures are not simply products of gravity-induced extension related to sediment-loading, diapirism, and gliding on mobile salt horizons at depth like occurred along the northern Gulf of Mexico and lower part of the Mississippian embayment (e.g., Worrall and Snelson, 1989). These fractures were produced by horizontal stresses whenever S_{Hmax} represents the principal stress direction.

Other fracture studies in Piedmont rocks, which are located well to the northwest of the Coastal Plain overlap in parts of the western Carolinas, indicate that only a few post-Alleghanian events are represented by fracture sets there (e.g., Garihan and Ranson, 1992; Garihan *et al.*, 1993). Still farther northwest, at the structural front of the fold-thrust belt in the Roanoke recess of Virginia only two post-Alleghanian events are documented (Bartholomew and Whitaker, in press). Hence, as our understanding of each of these 17 events, found near the Coastal Plain overlap, discussed in this paper grows regionally, we hope to be able to recognize their lateral geographic extent, to understand the causes of variations in orientations within each event, and ultimately to identify the principal factors related to plate movements and/or isostatic adjustments (e.g., Cronin, 1981; Hancock and Engelder, 1989) which caused these 17 post-Alleghanian events.

AGE CONSTRAINTS

Most of our work on Mesozoic and Cenozoic fractures in Georgia and South Carolina has focused on two different types of rocks: 1) fracture sets within Alleghanian granites (~300 Ma) and their crystalline host rocks of the Piedmont Province near the Coastal Plain overlap (e.g., Heath and Bartholomew, 1997; Bartholomew *et al.*, 1997a; Evans and Bartholomew, 1997, in press); and 2) Cretaceous-Quaternary strata of the Coastal Plain (e.g., Brodie and Bartholomew, 1997; Bartholomew *et al.*, 1997b, 2002, 2007). All fracture sets within the Alleghanian granites are necessarily post-crystallization and hence are post- (or possibly very late) Alleghanian (Evans and Bartholomew, in press). Radiometric age determinations for these granites (e.g., Dalmeyer et al., 1986), for "pink staining" (Kish, 1992), and for intrusion of diabase dikes (e.g., Sutter, 1988) all provide constraining ages for different fracture sets and mineralization events.

All fracture sets within Coastal Plain strata are necessarily the age of the enveloping strata or younger. Moreover, a fracture set found, for example, in Eocene and

older strata but not in younger strata, is constrained to be Eocene. But, near-surface syndepositional clastic dikes and/or growth faults that produced surface folds and influenced deposition of Coastal Plain sediments during the Late Eocene and Late Miocene more precisely constrain the age of some of these structural features (e.g., Bartholomew *et al.*, 2002). Also, orientations of orthogonal joints, which are in Pleistocene deposits of the Lower Coastal Plain of Georgia and South Carolina, that are consistent with S_{Hmax} and S_{Hmin} of the modern stress field suggest that these fracture sets probably developed in the current stress field (Bartholomew *et al.*, 2000).

Ages of different Cretaceous to Quaternary fracture sets in the crystalline rocks can be determined by correlation of the orientations of specific fracture sets within their relative age-sequence with those of successive ages in the sedimentary strata. Fracture sets in Piedmont country rocks (e.g., Eocambrian rocks at the Ridgeway Gold Mine; Secor *et al.*, 1986, 1998; Gillon *et al.*, 1998), into which Alleghanian granites were intruded, correlate well (via orientations, mineralization, etc) with those within Alleghanian granites, indicating that, regionally, all brittle fracture sets are of Mesozoic to Quaternary age.

FLUID INCLUSION MICROTHERMOMETRY

The presence of fluids during deformation and unroofing of orogenic belts is typically evidenced by mineralized (e.g., quartz, calcite) veins and fault zones that are parallel, or cross-cut, earlier deformed and/or metamorphic rock textures. Multiple deformation events, and hence multiple fluid events, may be recorded in cross-cutting structures and placed in a relative temporal sequence. These mineralized zones record the pressure-temperature and fluid history of the orogenic belt in the chemistry of vein minerals and within fluid inclusions which are trapped within vein minerals. Studies of

fluids inclusions and vein minerals provide significant information on fluid-rock interactions, evolution of fluid composition, and deformation processes that occur in exhumed terranes (e.g. Craw and Koons, 1989; Boullier, 1999; Evans and Battles, 1999; Evans, in press). In addition, analysis of fluid-inclusions provides information on, and changes in, pressure-temperature conditions during deformation and exhumation (e.g., Holm and others 1989; Craw, 1990; Jenkin and others, 1994; Evans and Bartholomew, in press).

We used fluid-inclusion microthermometry to characterize the chemistry and evolution of fluids which were present in Piedmont rocks during post-Alleghanian exhumation related to Mesozoic rifting. By using data from multiple, temporally controlled vein sets, we were able to establish a fluid history during exhumation.

We hope, eventually, to compare our Mesozoic to Cenozoic sequence of fracture sets, developed from our regional fracture-set data and fluid-inclusion data, with that from drill core recovered from beneath the USDOE Savannah River Site (Dennis *et al.*, 1997; Huner *et al.*, 1997) and with development of multiply deformed siliceous cataclastic zones in the Piedmont (e.g., Garihan and Ranson, 1992; Garihan *et al.*, 1993).

CONVENTIONS AND METHODS USED IN THIS STUDY

We used the same conventions as Bartholomew *et al.* (2007). Measurements, diagrams, and discussions of fracture attitudes all follow the right-hand convention, which is: strikes are from 001^{o} to 360^{o} and measured clockwise from north with the surface dipping to the right. Dips are measured from 001^{o} to 090^{o}, and pitches are measured from 001^{o} to 180^{o} from the strike direction. Joints are shown as rose diagrams and faults are shown on equal-area lower hemisphere stereographic projections. North

(N) is at the top of each diagram and strikes, which follow the right-hand convention, go clockwise from 1^{o}-360^{o} on all diagrams. The circle for each rose diagram is given as a percentage (in parentheses) of the total number of joints. Because the rose diagrams use data with the right-hand convention, they can be used to interpret if part of a fracture set (say, NNE-striking, ESE-dipping joints) was later preferentially mineralized or reactivated as high-angle faults versus another part (SSW-striking, WNW-dipping joints) which preserves the original joint characteristics.

The type of displacement on fault surfaces was determined (where possible) from offset points on small faults and from fault-surface features following criteria of Petit (1987). Fracture sequences at sites are developed by establishing the relative age relationships of fracture sets (i.e. related joints and faults) based on orientations and *en echelon* patterns, intersection relationships, surface features (e.g., plumose, pinnates, slickenlines), mineralization (if present) sequence, slip-vectors and reactivation history of joints and faults.

Mineralization on fracture surfaces is indicated by using abbreviations (e.g., **ch** for chlorite; **hem** for hematite). Thus, **ch**-joints are joints that are coated with chlorite and **ch**-faults are faults that are coated with chlorite with slickensides which post-date **ch**-mineralization. A sequence of mineralization on a surface is given from oldest to youngest [e.g., pink-staining (**PS**) followed by **ch** + **ep** is **PS\ch+ep** or **ch** followed by **hem** followed by laumontite (**lau**) followed by calcite (**cal**) is **ch\hem\lau\cal**].

Fluid inclusion assemblages (Goldstein and Reynolds, 1994) in 100-200-μm thick, doubly polished, thin section plates were mapped (Touret, 2001) and characterized as to their probable origin as primary, pseudosecondary, or secondary; and as to which stage of mineralization they occurred in, as well as their location within the mineral crystal (e.g. core, terminus, etc.). Conventional heating and freezing microthermometric analyses were performed using a modified U.S. Geological Survey-type heating-freezing

stage manufactured by FLUID Inc. The stage was calibrated at 0°C (ice bath), 374.1°C (critical point of water), and -56.6°C (CO_2 triple point) (the latter two standards supplied by SYNFLINC, Inc.).

Estimates of fluid composition were made using the computer program FLUIDS (Bakker, 2003; Bakker and Brown, 2003). Isochores for H_2O – NaCl inclusions were determined from the equation of state presented by Bodnar and Vityk (1994). Salinities for the H_2O – NaCl inclusions were calculated using the equation presented by Bodnar (2003). For inclusions containing carbon dioxide ± methane, trapping temperature and pressure were determined from isochores and phase relationships for the carbon dioxide-methane system (Duan, Møller and Weare, 1992a, 1992b). For H_2O-CO_2-NaCl inclusions isochores were determined using the equation of state presented by Bowers and Helgeson (1983). In the CO_2-bearing aqueous inclusions, salinity was derived from the dissociation temperature of the clathrate (T_{mcl}) in the presence of CO_2-liquid and vapor (Diamond, 1992).

FIELD-TRIP STOPS

Stop 1. Columbia Quarry, Vulcan Materials Company, Columbia, SC (*Figures 2* and *3*).

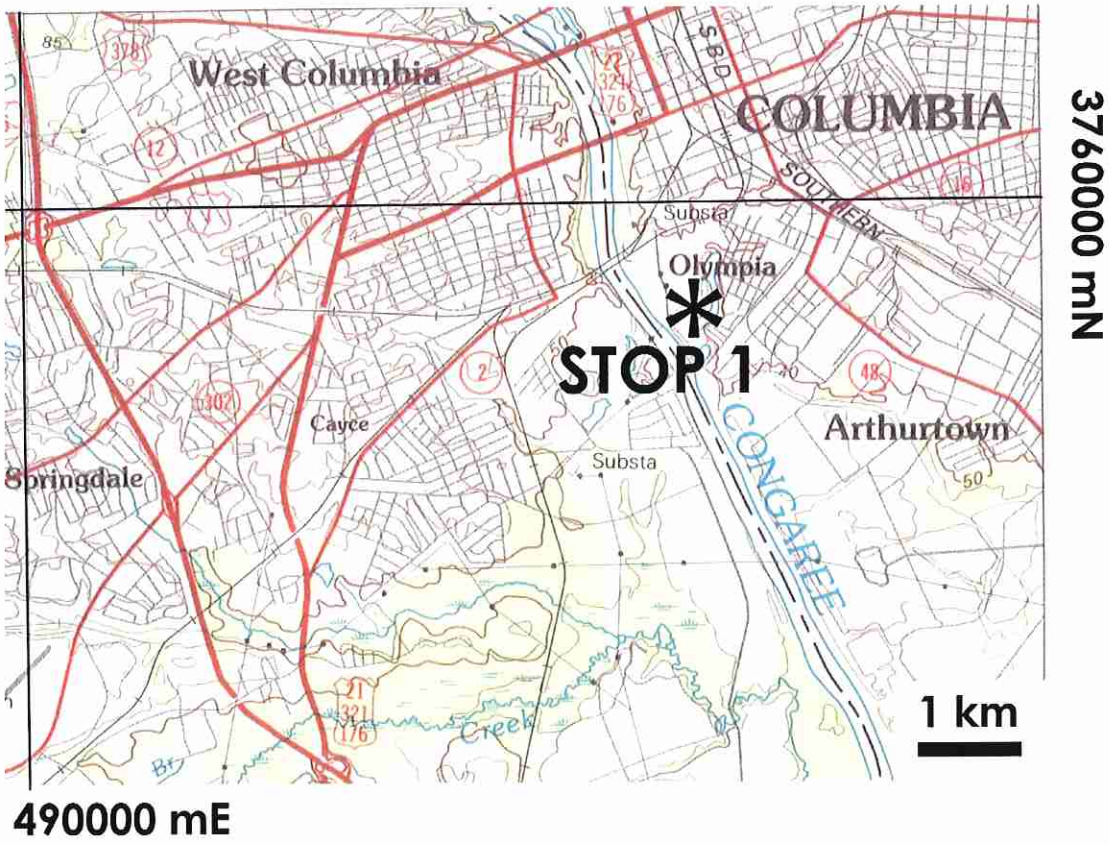

Figure 2. Map showing location of STOP 1 in the NE- part of the Aiken, SC-GA, 1:100,000-scale quadrangle. Contour interval is 10-m.

The Columbia Quarry (STOP 1; *Figures 2* and *3*) and the Martin Marietta Cayce Quarry across the river as well as the Lake Murray Spillway (STOP 7) represent one of the first areas of crystalline rocks we analyzed (Heath, 1996) because we could see what specific fracture sets looked like both near the surface, where weathering and groundwater affected fracture surfaces, and at depth where Mesozoic mineralization was more frequently preserved. At shallow depths (~0-50-m), limonite and manganese oxides are common mineralization, but the same fractures at depth may be non-mineralized

(**NM**) or **PS**, **hem**, **lau**, and **cal** may occur. A greenschist-facies mineral assemblage (**ch+qtz+py**) is associated with the earliest veins and normal faults. Subsequent mineralization on new favorably oriented fractures was **PS\hem+/-ep\cal**. Laumontite (**lau**) both preceded and post-dated **hem**. For this trip, we are only looking at Mesozoic fracture sets in the crystalline rocks and Cretaceous-Quaternary fracture sets in Coastal Plain strata. We will not discuss the Cretaceous-Quaternary fracture sets in the crystalline rocks, which were partially discussed by Bartholomew *et al.* (1998, 2007).

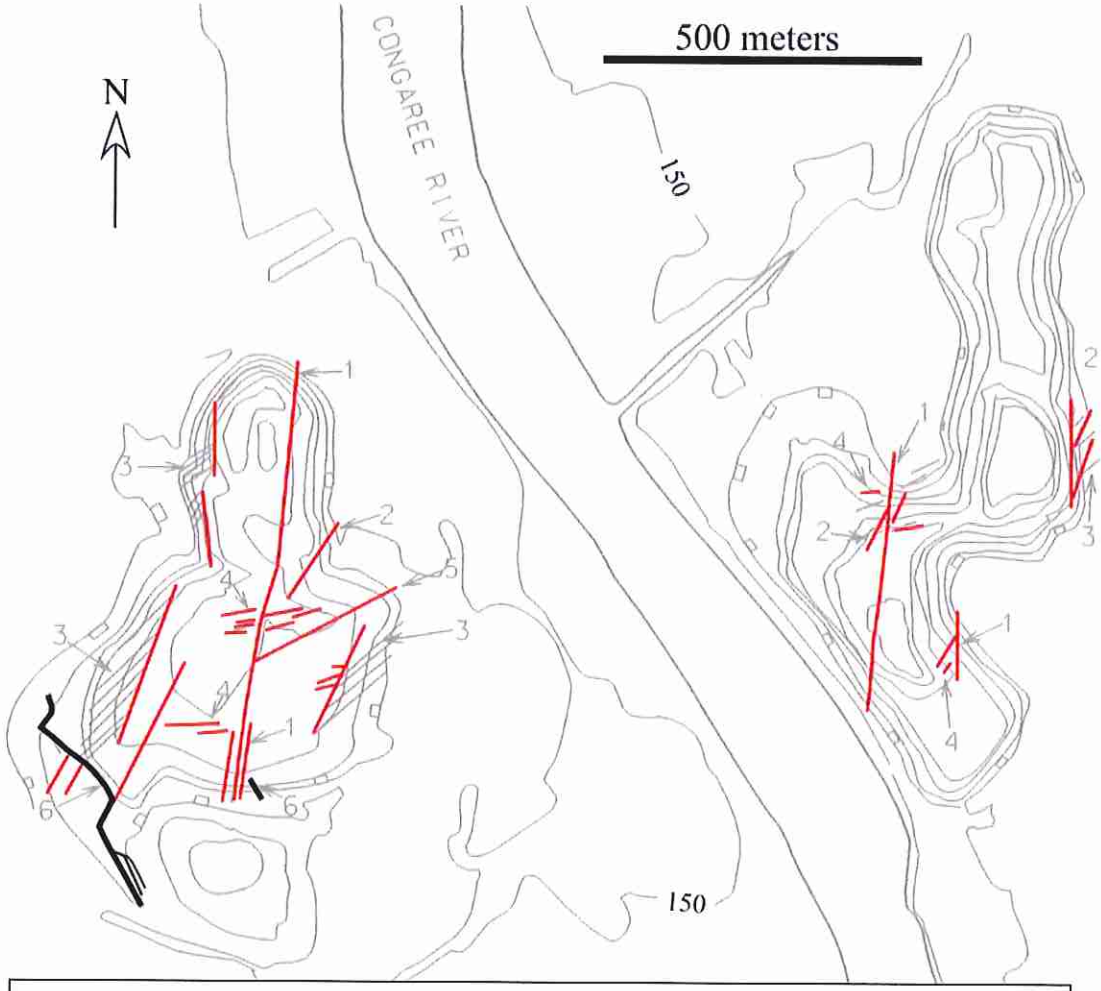

Figure 3. Map showing major fracture sets mapped in 1996 in the Vulcan Columbia Quarry (east of the Congaree River) and the Martin Marietta Cayce Quarry (west of the river). 1: N-S-trending fault zones; 2: NNE-trending fault zones; 3: NE-trending TR6 joint set; 4: E-W-trending fault zones; 5: NE-trending fault zone; 6: NW-trending diabase dikes. Contour interval is 50 feet. Modified after Heath (1996).

The oldest set of fractures (*Figure 4*) is the set of ENE-trending oblique-normal faults (**TR1**) with a slip-vector of ~215^{O}) and with a greenschist-facies mineral assemblage (**qtz+ch+py**). This set of faults is consistent with similarly oriented **TR1** faults and small quartz veins at both the Ridgeway Gold Mine (Bartholomew *et al.*, 1998) and the Augusta Quarry (Bartholomew *et al.*, 2007) (*Figure 1*). Bartholomew *et al.* (1998) suggested that higher (residual) temperatures, lower $f\,O_2$, and low Fe-content are responsible for the development of this **ch**-assemblage prior to the onset of widespread circulation of hydrothermal fluids responsible for **PS** on most subsequent joint sets. **TR1** is consistent with an interpretation that these dip-slip normal faults formed during Triassic initiation of SW-NE-trending extension along the SE-striking segment of the Suwannee-Wiggins suture across eastern Georgia (**Figure 1**).

The next two younger fracture sets (**TR2** and **TR3**) also are interpreted to have formed during failed rifting (N-S- to NNW-SSE-extension) along the Suwannee-Wiggins suture. However, these fracture sets are characterized by extensive **PS** followed by some later **lau**, **hem**, and/or **cal** mineralization. Mauldin et al. (1997) attributed **PS** in core beneath the US DOE Savannah River Site to hydrothermal alteration of calcic feldspar by potassic fluids and Kish (1992) dated **PS** from core at 220 +/-4 Ma. This age suggests that **TR2** and **TR3** developed early in the late Triassic. The trend of **TR2** here is similar to **TR2** orientations at both the Ridgeway Gold Mine and the Augusta Quarry (Bartholomew *et al.*, 1998, 2007). However, **TR3** was not noted at the Ridgeway Mine and is only a minor trend at the Augusta Quarry.

PS\hem TR4 and **TR5** are also found at the Augusta Quarry (Bartholomew *et al.*, 2007; their **TR3A** and **TR3B**) where a later static t**alc** mineralization also occurred on pre-existing, SSW-trending joints (equivalent to **TR4**). In the Columbia quarries (*Figure 3*), **lau** (*Figure 5*) occurs frequently on these fractures as both pre- and post-**hem**. But both **hem** and **lau** always pre-date **cal** (*Figure 6A, B*, and *C*).

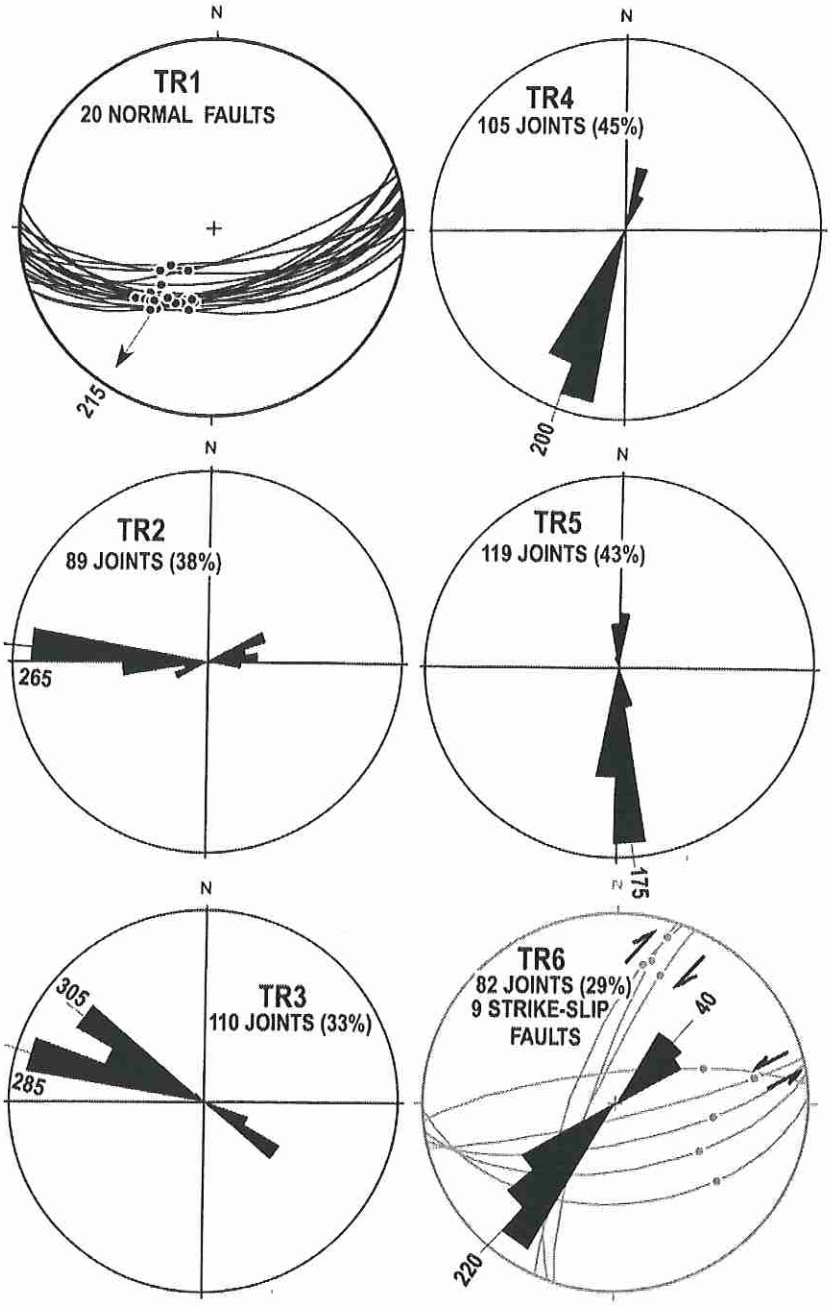

Figure 4. Triassic fracture-set sequence consists of:

- ***A: TR1-*** *ENE-trending, oblique-normal faults with* ***qtz+/-ch+/-py assemblage;***
- ***B: TR2-*** ***W****-trending,* ***PS*** *joints;*
- ***C: TR3-*** *NW-trending* ***PS*** *joints;*
- ***D: TR4-*** *SSW-trending* ***PS\lau\hem\cal*** *joints;*
- ***E: TR5-*** *S-trending* ***PS\lau\hem\cal*** *joints;*
- ***F: TR6-*** *SW-NE-trending* ***PS\lau\hem\cal*** *joints; and associated strike-slip faults along reactivated TR2 and TR4 joints.*

TR4 and **TR5** have the same trend as both the northern part of the basin-bounding Jonesboro fault of the Deep River Basin in NC (*Figure 1*) and the oldest set of syndepositional joints and associated clastic dikes within that Triassic basin (Wooten *et al.*, 2001). This indicates that **TR4** and **TR5** developed as syndepositional systems during the late Triassic. These fracture sets also served as the dominant trend of fractures with **hem**, **lau**, and **cal** mineralization (*Figure 5* and *6B*).

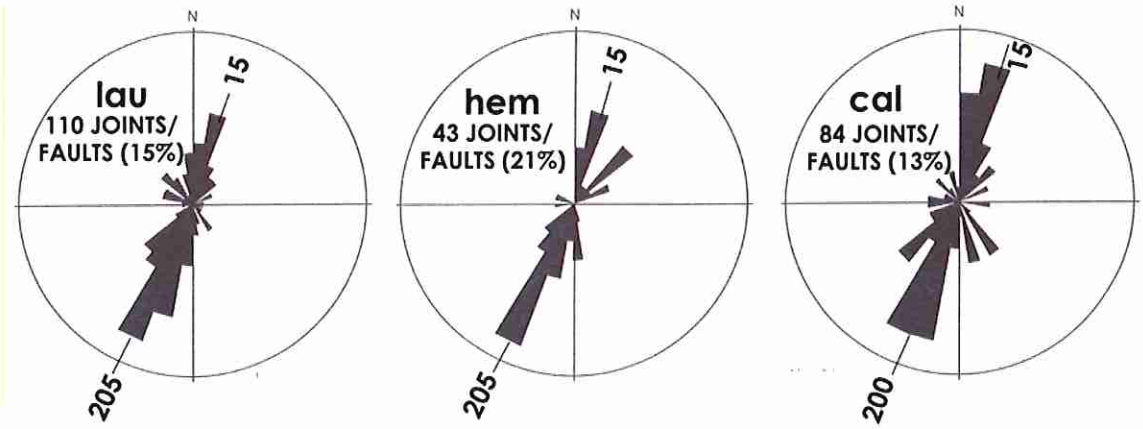

Figure 5. Rose diagrams showing the orientations of mineralized fractures observed in the quarries (STOP 1; Figures 2 and 3) and in the Lake Murray Spillway (STOP 7; Figures 24 and 25). ***lau****: laumontite;* ***hem****: hematite;* ***cal****: calcite. Modified after Heath (1996).*

TR6 is present at both the Ridgeway Mine (Bartholomew *et al.*, 1998; their **TR4**) and the Augusta Quarry (Bartholomew *et al.*, 2007; their **TR5A** and **B**). It also trends parallel to the basin-bounding fault of the subsurface Dunbarton Basin in South Carolina as well as to a segment of the Jonesboro fault (*Figure 1*) in North Carolina. The next younger set of syndepositional joints and clastic dikes within the Deep River Basin also trend NE-SE. Thus, **TR6** is an integral part of the late Triassic syndeposition fracture systems. **TR6** is generally characterized by **PS** (*Figure 6A*), although **hem** is present on some **TR6** fractures (*Figure 5*). Some **TR4** joints are reactivated as right-lateral strike-slip **TR6** faults.

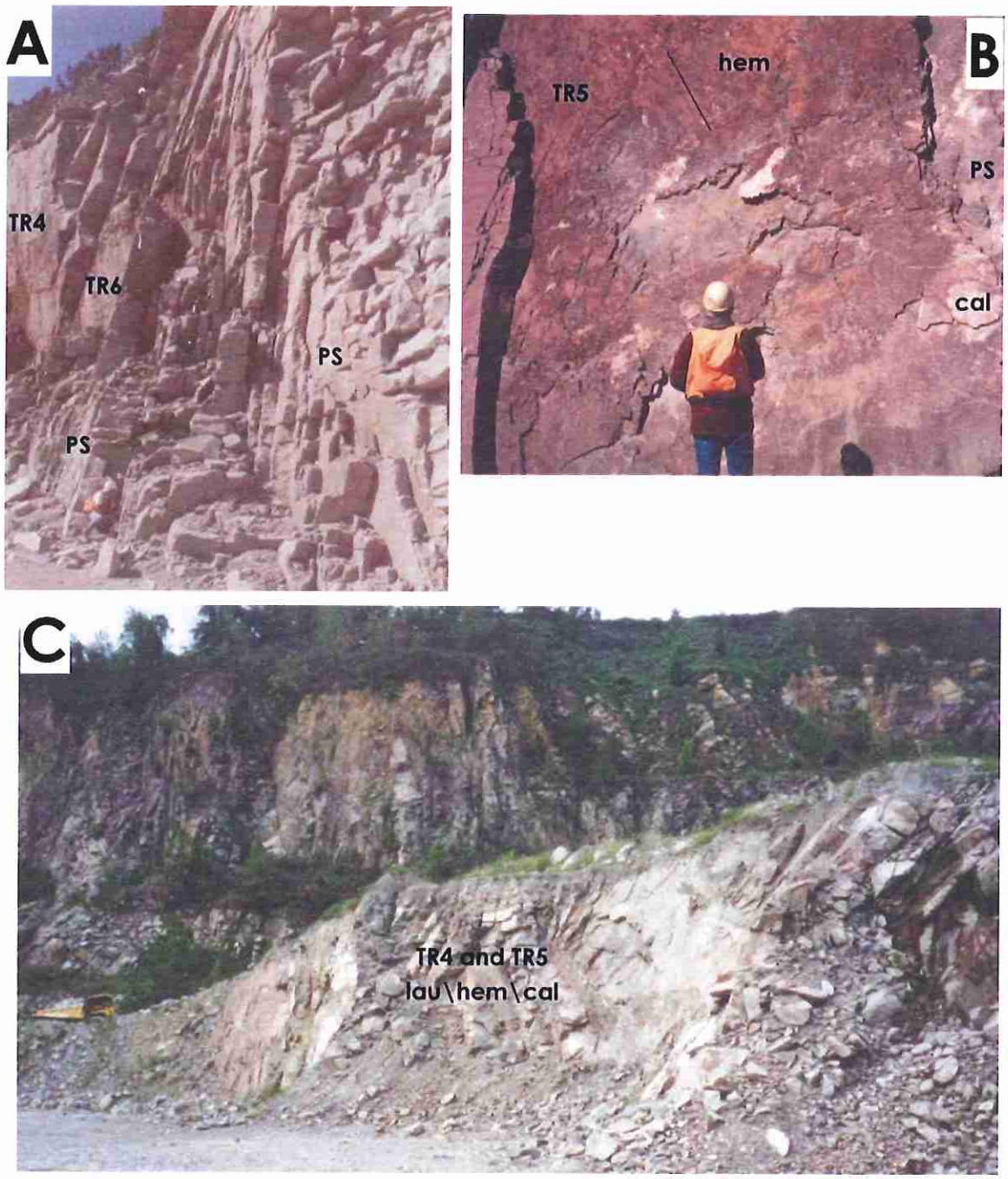

Figure 6. Typical mineralized joints of the quarries.

*A: Set of **TR6 PS** joints which terminate against a **PS TR4** joint which was reactivated as a fault (in NW-part of quarry west of the river).*
*B: **TR4 PS** joint subsequently reactivated first as a **hem** obique-slip fault (black line indicate slickenlines) and second as a **cal** joint (in NW-part of quarry west of the river).*
*C: In the foreground are both **TR4** and **TR5 PS** joints with **lau\hem\cal** mineralization (in SW-part of quarry east of the river).*

JR1 faults (*Figure 7A*) developed as left-lateral and right-lateral strike-slip faults along reactivated **TR4** and **TR5** joints, respectively (*Figure 8*). **TR4** joints were also reactivated as left-lateral strike-slip faults (*Figure 8*) along with **TR3** joints reactivated as right-lateral strike-slip faults as part of **JR2** (*Figure 7B*). A large set of NW-SE-trending joints developed during **JR2** and diabase dikes, in the quarry to the west of the river (*Figure 3*), also follow this trend which is the dominant regional dike trend (e.g., Ragland et al., 1983). **JR2** faulting typically post-dated **hem** and **lau** mineralization, whereas most **cal** mineralization post-dated **JR2**. **JR2** joints are typically **NM**, but may have spotty **hem+lau**. The large diabase dike (*Figure 3*) is bordered by a large calcite vein and is cross-hatched with small calcite veins indicating **cal** mineralization occurred during **JR2**.

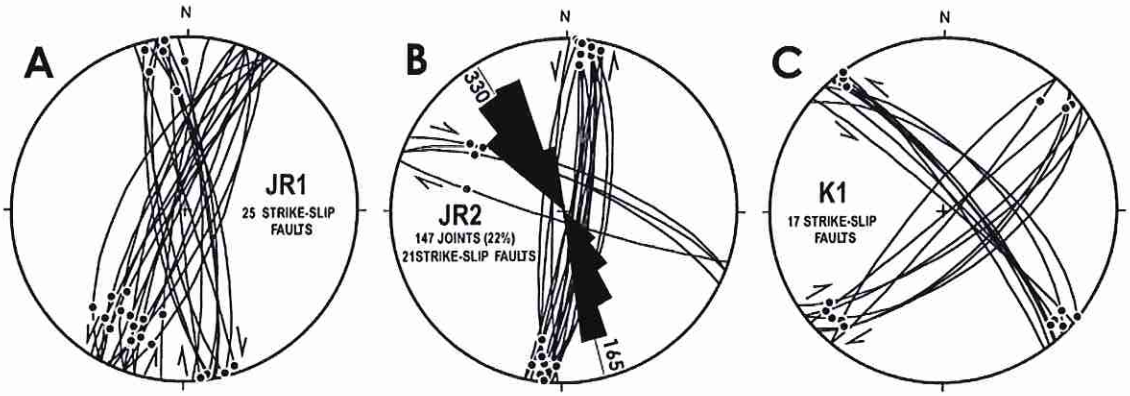

Figure 7: Jurassic to Cretaceous fracture-set sequence consists of:
*A: **JR1**- Strike-slip faults along reactivated **TR4** and **TR5** joints;*
*B: **JR2**- NW-trending joints associated with diabase dikes and strike-slip faults along reactivated **TR3** and **TR4** joints;*
*C: **K1**- Strike-slip faults along reactivated **TR3**, **JR2**, and **TR6** joints.*

Cretaceous faults developed as NW-trending, left-lateral strike-slip faults along reactivated **JR2** and **TR3** joints and as SW-trending, right-lateral strike-slip faults along reactivated **TR6** joints (*Figure 7C*).

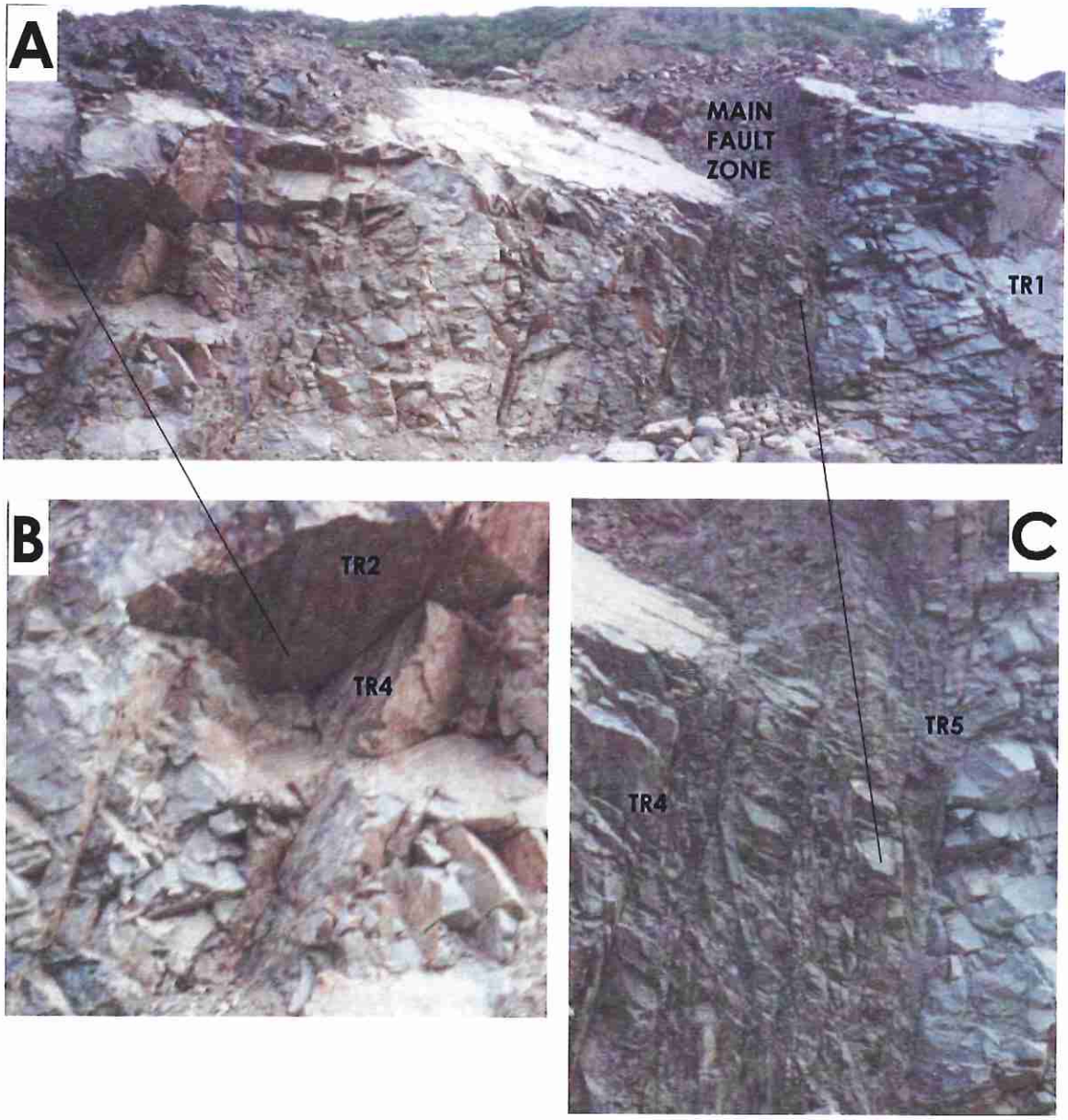

Figure 8.The maim N-S-trending fault zone in Vulcan Columbia Quarry.

A: View looking north at the main N-S-trending fault zone in the western part of the quarry.
*B: Closeup of S-trending **TR4 PS** joints reactivated as part the fault zone adjacent to a **TR2** joint.*
*C: Closeup of main fault zone bounded on east and west, respectively by fault-reactivated **TR5** and **TR4 PS** joints.*

Fluid Inclusions

Most of the veins at these two quarries are late N-S to NNE-SSW-striking veins that are mineralized with **cal** ± zeolites (**Z**) ± **ch** (*Figures 9 and 10*). Two early quartz veins that were later reopened are included.

The early quartz contains secondary two-phase aqueous (*Figure 9A*) with homogenization temperatures of 229° to 239°C and salinities of 0.0 to 3.6 wt. % NaCl equivalent. The inclusions also contain minor CO_2, as evidenced by formation of a CO_2 clathrate upon freezing. Pressure corrected trapping conditions are a minimum of 250°C and 30 MPa at hydrostatic conditions, and a maximum of approximately 400°C and 250MPa at near lithostatic conditions (*Figure 9B*). The upper bounds are based on CO_2-rich inclusions from veins in nearby localities. The early quartz was therefore trapped at a depth of 3.0-9.6-km. Calcite mineralization found in the later veins and in the reopened quartz veins contains only primary and secondary two-phase aqueous inclusions (*Figures 9B* and *9C*) with homogenization values of 76° to 126°C. Salinity is always 0.0 wt. % NaCl equivalent, suggesting meteoric influx. Pressure corrected trapping conditions give a temperature range of 80° to 145°C, and a pressure range of 8 to 40 MPa (*Figure 9B*). These conditions correspond to a trapping depth of 0.8-4.0-km depending upon the geothermal gradient.

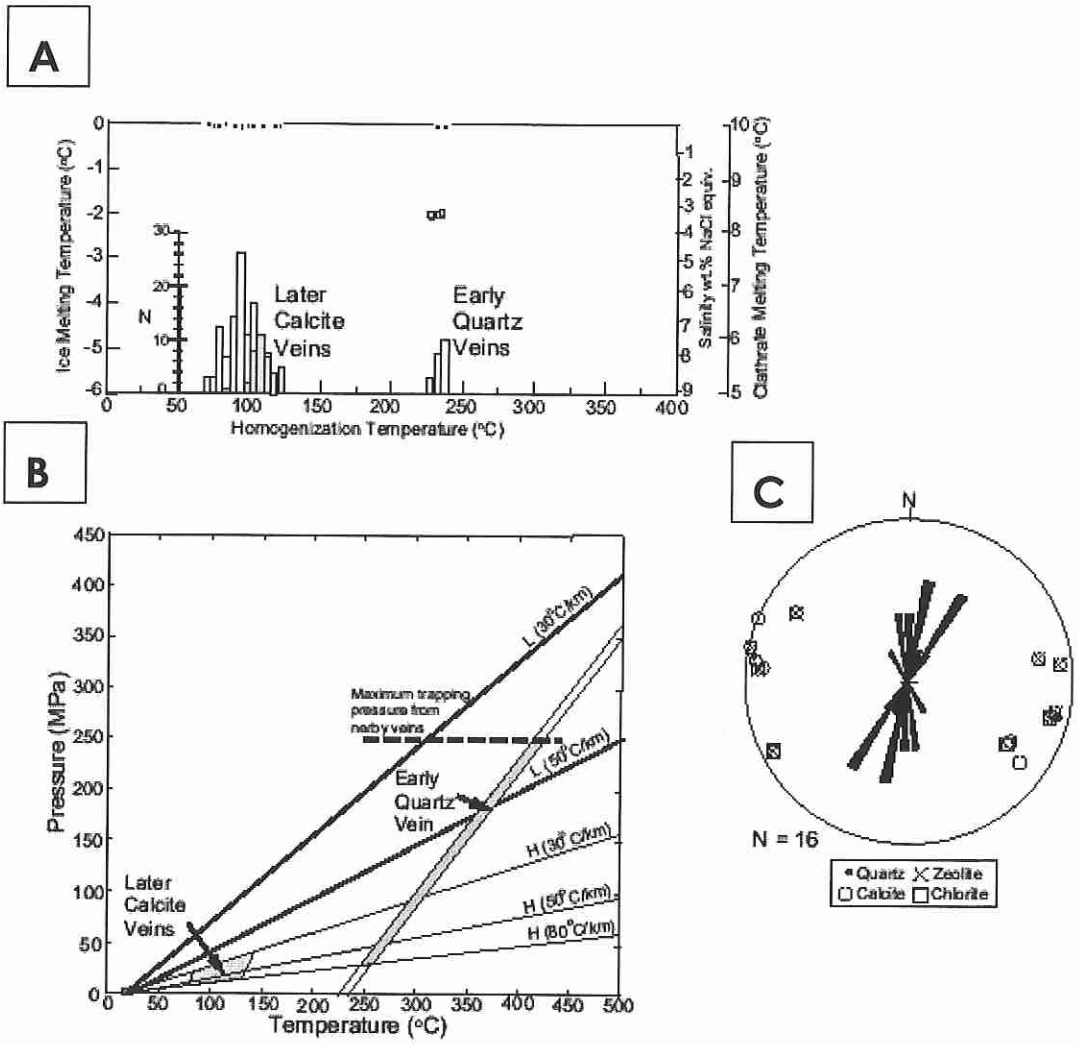

Figure 9

A: Summary of fluid inclusion data from veins at quarries (Figure 3). N is number of data.

B: P-T diagram showing trapping conditions for fluid inclusions in veins at quarries. Also shown are lithostatic (L) and hydrostatic (H) thermobaric gradients for various geothermal gradients.

C: Lower hemisphere equal area stereo net showing orientations of veins used for fluid inclusions microthermometry and vein petrography. Symbol used for pole to veins show types of mineralization present.

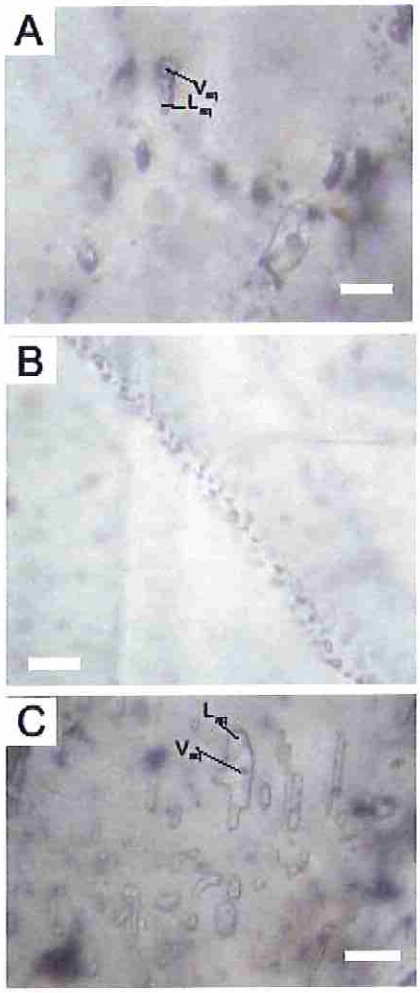

Figure 10. Photomicrographs of fluid inclusion types found in veins in the southeastern Piedmont:

A: Secondary two-phase H_2O-NaCl inclusions in quartz showing liquid water (L_{aq}) and water vapor (V_{aq});
B: Two-phase secondary H_2O fluid inclusion plane in a calcite vein;
C: Primary two-phase H_2O inclusions in a calcite vein. Scale bar is 10 microns.

Stop 2. Road cut near Woodlawn, McCormick County, SC (Figure 11)

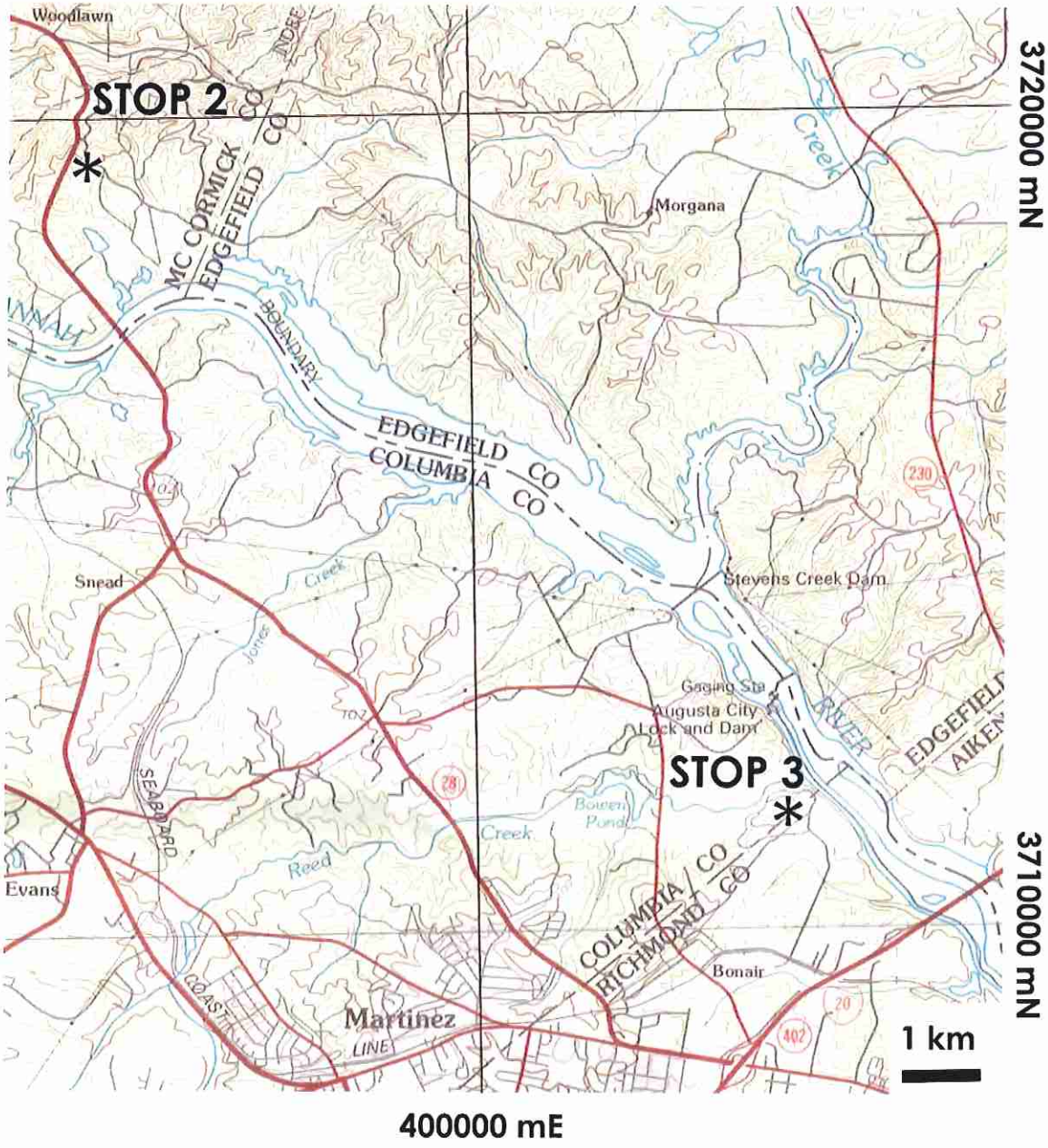

Figure 11. Map showing locations of STOPS 2 and 3 on a part of the Clark Hill Lake, GA-SC 1:100,000-scale quadrangle. Contour interval is 10-m.

This roadcut is located on the north side of a secondary road just east of its intersection with SC State Road 28 about 2-miles south of Woodlawn, SC (*Figure 11*). This exposure contains excellent examples of small reverse faults offsetting pegmatites in granite. Because of the proximity of this exposure to the Augusta quarry of Martin Marietta Materials (*Figures 11 and 12A*), most of the structures observed here can be correlated with Late Eocene and Late Miocene structures observed in the quarry and related to repeated reactivation of the Belair fault zone (e.g., Prowell and O'Conner, 1978; Bramlett *et al.*, 1982; Bartholomew *et al.*, 2007). Five joints and 1 normal fault (*Figure 12B*) are likely Triassic fractures, but are too few in number to correlate with specific sets identified by Bartholomew *et al.* (2007).

Three reverse faults (*Figure 12C*) are identified as belonging to the first phase of late Eocene deformation (**E1**). The slip-vector of 110^{O} for **E1** is the same as that documented in the quarry (Bartholomew *et al.*, 2007) and identified earlier by Prowell and O'Conner (1978) for the Belair fault zone (*Figure 12A*). The three faults identified in this road cut are likely favorably oriented (Sibson, 1990) Triassic faults which were reactivated in the Eocene as noted by Bartholomew *et al.* (2009).

Nine reverse faults (*Figures 12D* and *E*) are identified as belonging to the first phase of Late Miocene deformation (**M1A** and **M1B**). Prowell and O'Conner (1978) also identified a second slip-vector of 155^{O} on the Belair fault zone and this correlated with the 153^{O} slip-vector for **M1A**. Although **M1A** and **M1B** could be plotted together they each represent approximately dip-slip on faults of slightly different orientation which suggests about 10^{O} clockwise rotation of S_{Hmax}. S_{Hmax} for **M2** is approximately 35^{O}-215^{O} which is similar to that documented by Bartholomew et al. (2007) in the Augusta quarry and in other localities in the Coastal Plain. Thus here, as elsewhere in the SC-GA area, S_{Hmax} appears to undergo a 60^{O} clockwise rotation during late Miocene deformation.

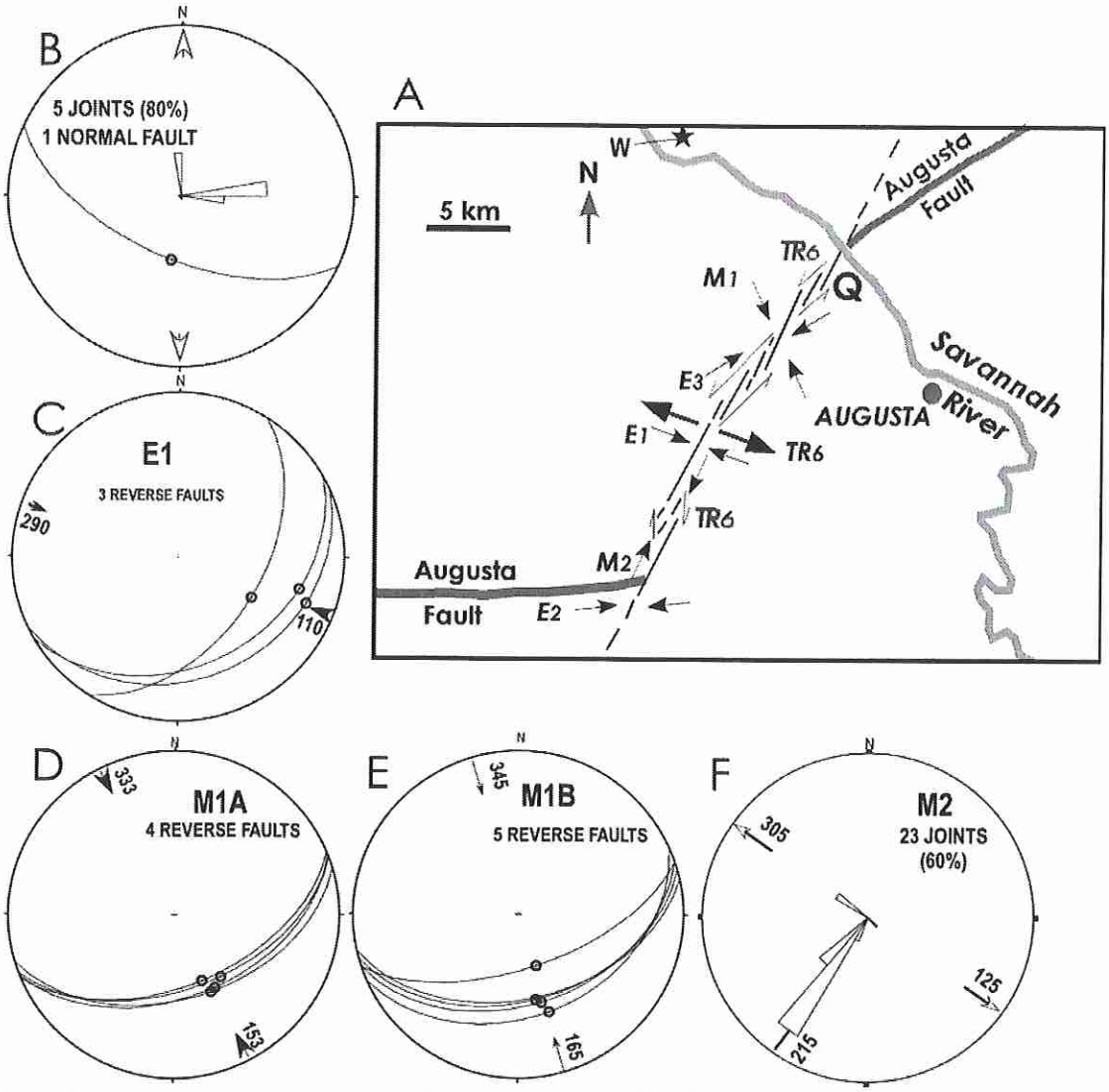

Figure 12 Eocene and Miocene fracture sets and Woodlawm, SC (Figure 11).

*A: Location of Woodlawn STOP 2 (W) relative to the Augusta Quarry (Q), the Augusta fault and the NE-trending Belair fault zone which developed during **TR6** and was reactivated during Eocene and Miocene deformation.*
*B: Early fractures which may represent parts of **TR2**, **TR3**, and **TR5**.*
*C: **E1** reverse faults.*
*D: **M1A** reverse faults.*
*E: **M1B** reverse faults.*
*F: **M2** joints with a dominant trend of 215^{o}.*

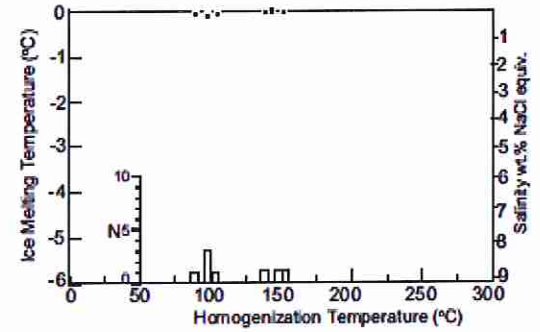

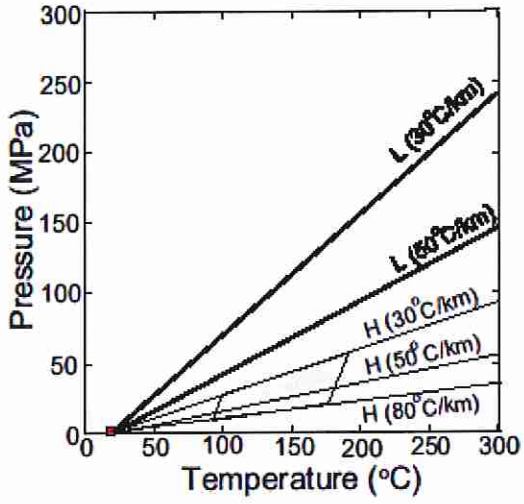

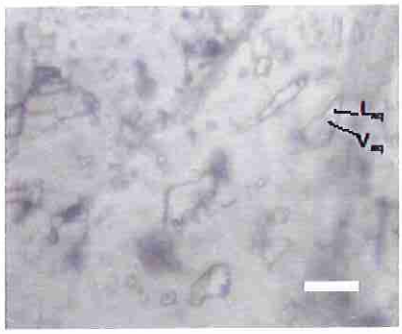

Figure 13. Fluid inclusion data at STOP2 (Figure 11).
A:. Summary of fluid inclusion data from STOP 2. N is number of data.
B: P-T diagram showing trapping conditions for fluid inclusions in CHL-5-1A. Also shown are lithostatic (L) and hydrostatic (H) thermobaric gradients for various geothermal gradients.
C: Photomicrograph of secondary aqueous fluid inclusions in the CHL-5-1A vein. Scale bar is 10 microns.

A single quartz vein (300/90) from this site has secondary two-phase aqueous inclusions (Figure 13) that homogenize between 90° and 164°C, with ice melting temperature of 0.0°C, indicating pure water (Figure 13B). Pressure corrected trapping conditions are 95° and 175°C and 10 to 55 MPa (Figure 13B). These inclusions were trapped at some point during exhumation, with a fluid trapping depth of between1.0 to 5.5 km depending on the geothermal gradient. Although no primary inclusions were found in this vein, veins from nearby sites have primary aqueous and carbonic inclusions that give trapping conditions of up to 400°C and 215MPa, suggesting that the vein formed at a depth of over 8 km.

STOP 3. Augusta Quarry, Martin Marrieta Materials, Augusta, County, GA (*Figure 11*).

We will use a handout of the Augusta Quarry STOP from Bartholomew *et al.* (2007) courtesy of Georgia southern University.

STOP 4. Abandoned clay pit on north side of road between Graniteville and Aiken, Aiken County, SC (*Figure 14*)

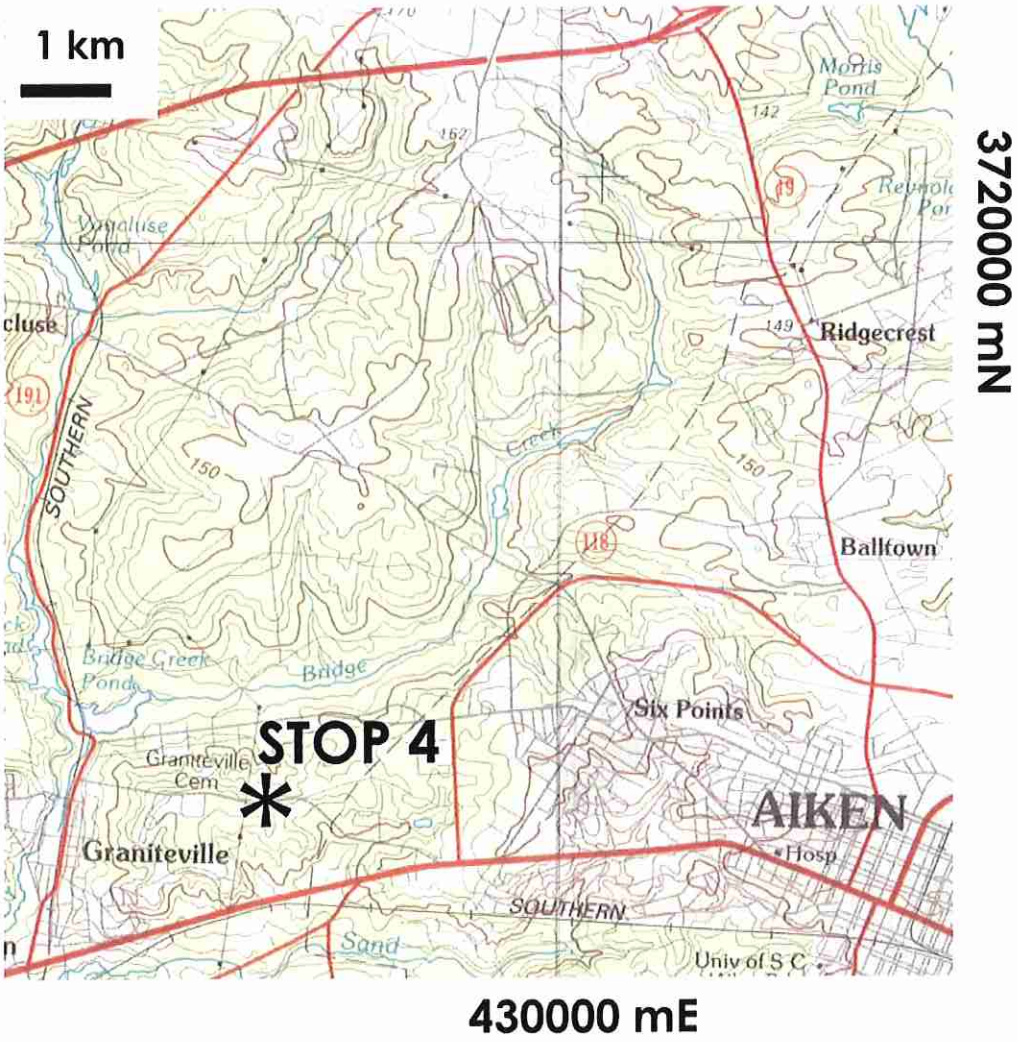

Figure 14. Map showing location of STOP 4 on a part of the Aiken SC-GA 1:100,000-scale quadrangle. Contour interval is 10-m.

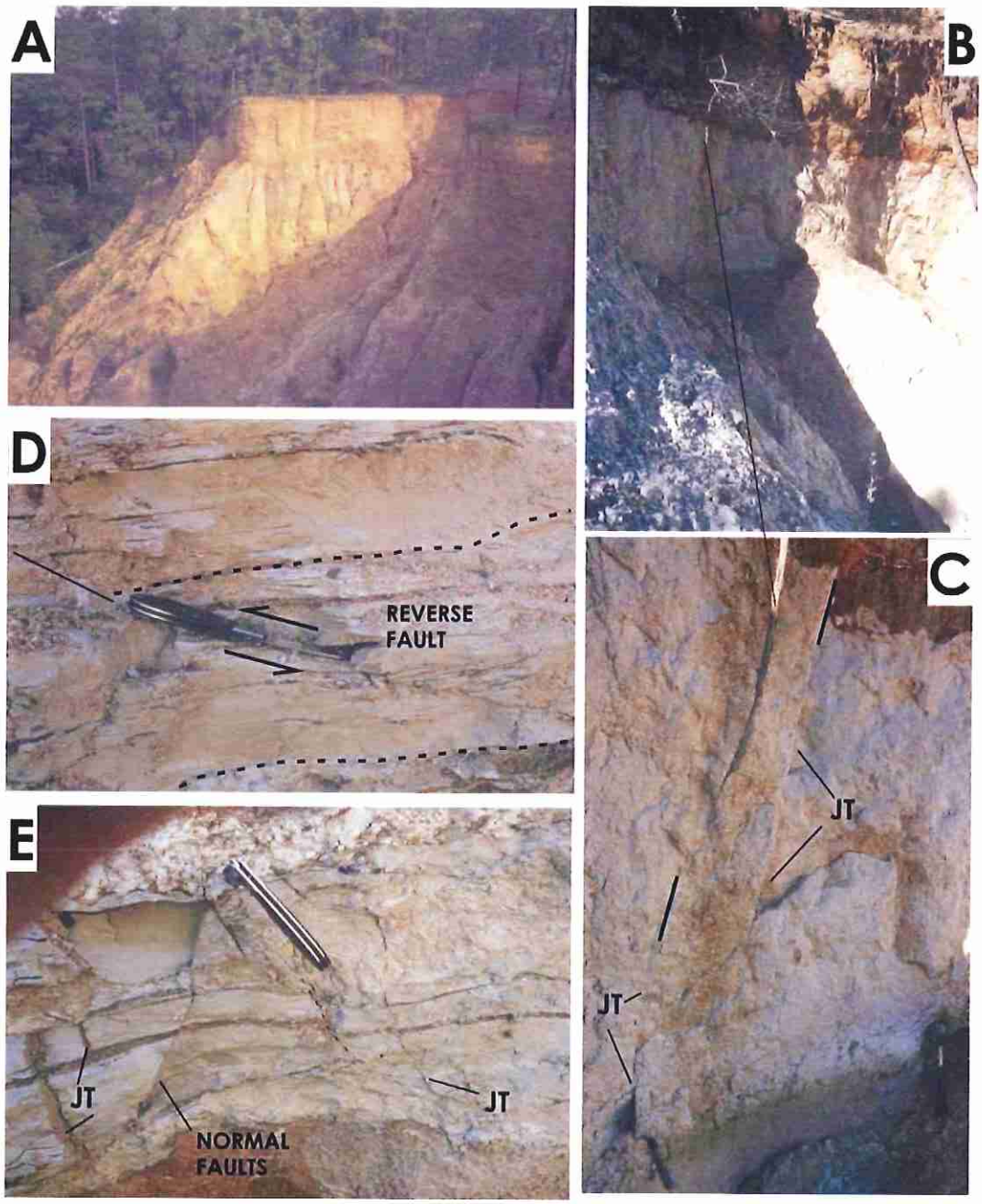

Figure 15. Photographs of fractures in clay pit at STOP 4.

A: Typical weathered exposure in which fractures be most visible.
B: Closeup the head of a gulley in which fractures were measured.
C: Closeup of area in B with two steeply dipping, 1-meter-high joints (black lines mark the top of each joint).
D: Closeup of small thrust fault; dashed line marks the base of an offset bedding plane; knife-handle is about 9-cm-long.
E: Closeup of small normal fault and joints

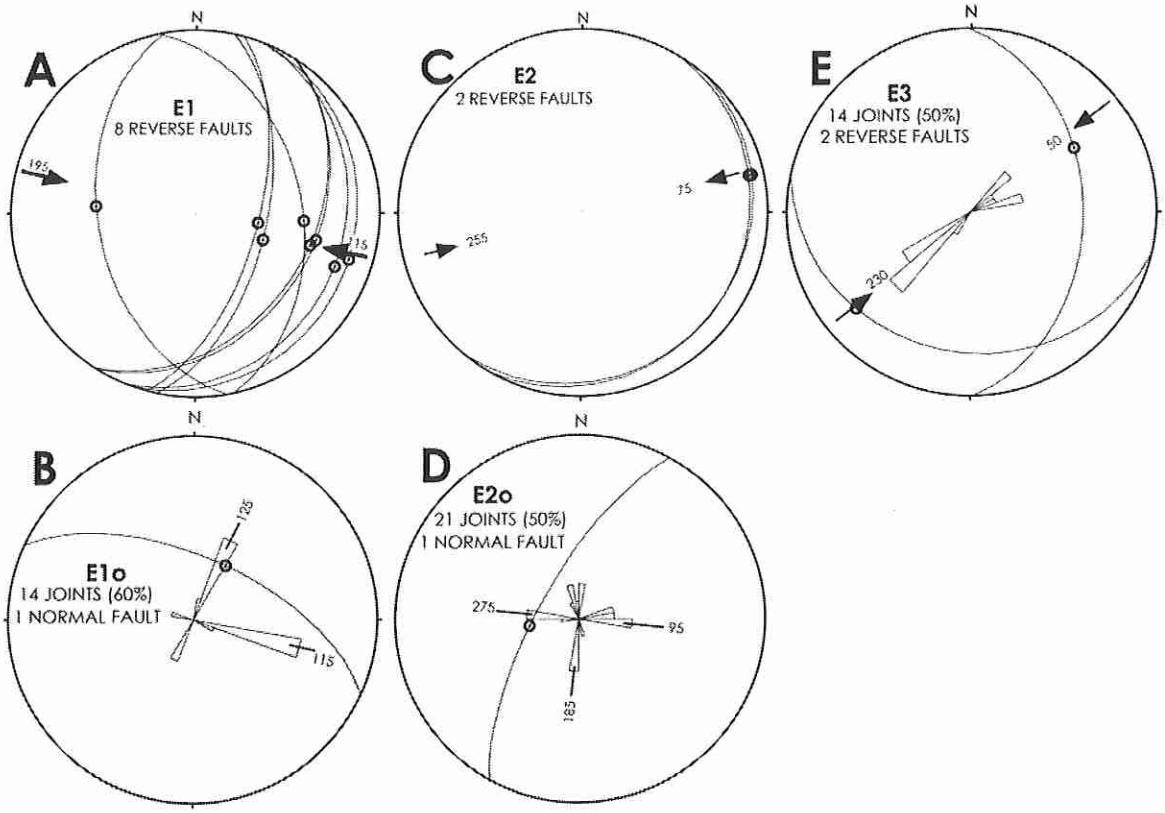

Figure 16. Eocene fracture sequence consists of:

A: E1- Reverse faults indicative of WNW-trending S_{Hmx}. at about 115^{O}
B: E1o- Orthogonal joint sets and 1 normal fault related to E1
C: E2- Reverse faults indicative of WNW-trending S_{Hmx}. at about 75^{O}
D: E2o- Orthogonal joint set and 1 normal fault related to E2
E: E3- Reverse faults and joints indicative of NE-trending S_{Hmx}. at about 50^{O}

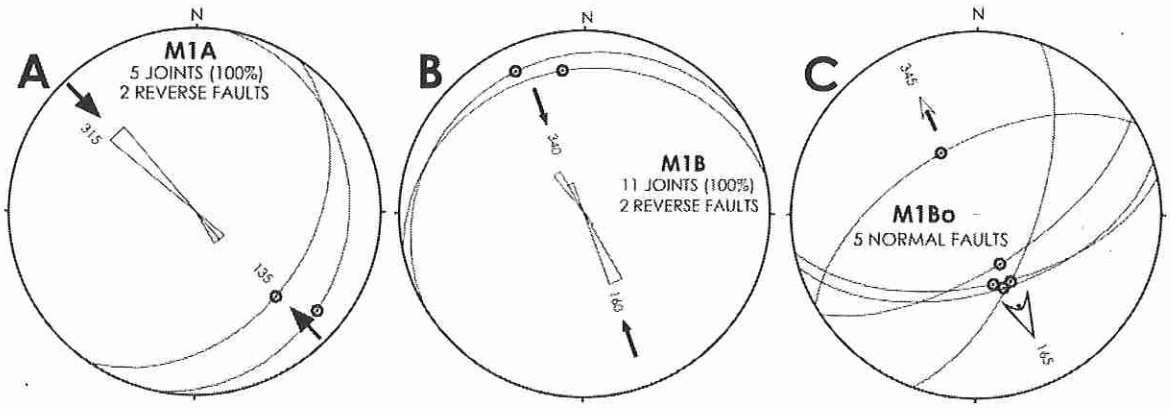

Figure17. Miocene fracture sequence consists of:

A: M1A- Reverse faults and joints indicative of NW-trending S_{Hmx}. at about 135^{O}
B: M1B- Reverse faults and joints indicative of NW-trending S_{Hmx}. at about 160^{O}
C: M1Bo- Orthogonal set of normal faults indicative of NW-trending S_{Hmin} at about 165^{O}

STOP 5. Road cut near Tinker Creek near Williston, Barnwell County, SC (*Figure 18*)

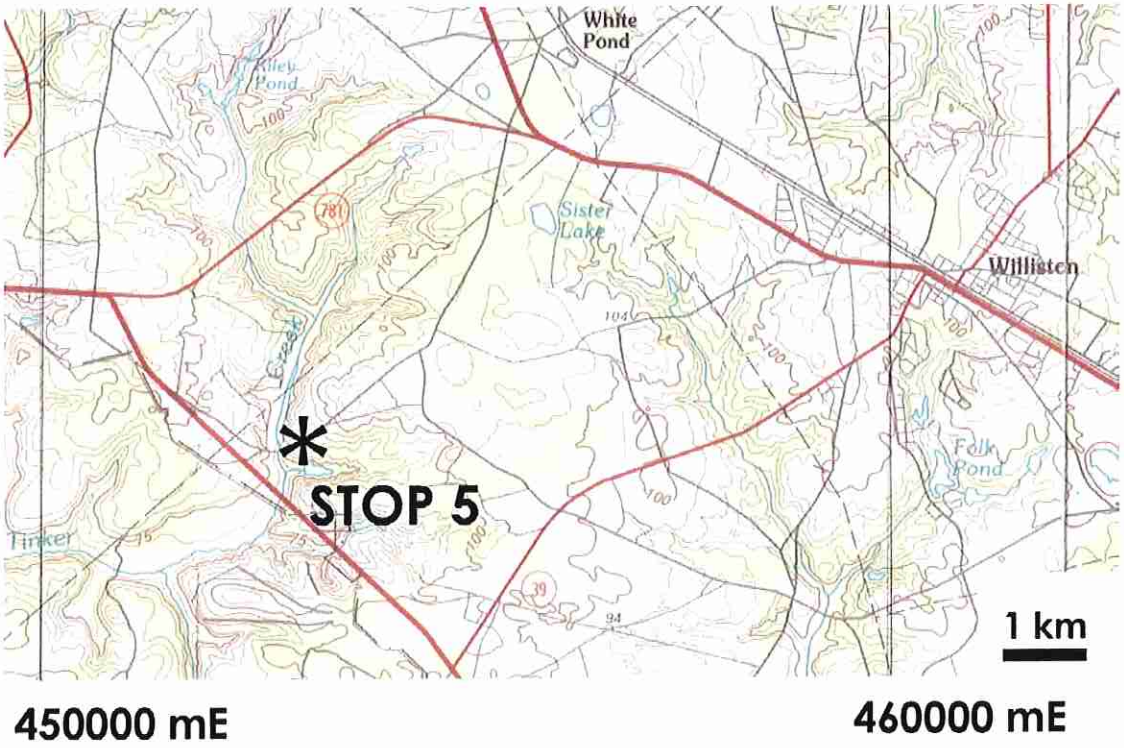

Figure 18. Map showing location of STOP 5 on a part of the Barnwell, SC-GA 1:100,000-scale quadrangle. Contour interval is 5-m.

The main reverse fault and adjacent syncline (*Figure 19A* and *B*) in the upper Eocene Tobacco Road Sand at this stop was previously discussed by many researchers (Colquhoun et al., 1982; McDowell and Houser, 1983; Willoughby and Nystrom, 1994; Willoughby and Clendenin,1995) and these syndepositional structures were subsequently analyzed by Bartholomew *et al.* (2002). This is one of the few localities in the Coastal Plain where a then-active Eocene fault (*Figure 19B*) was demonstrably shown to have had surface expression even though its offset is small (0.2-0.3m). The syndepositional faulting produced a small arch which was subjected to erosion while the adjacent syncline was filled with detritus which included material eroded from the arch.

Figure19. Williston structure.

A: Composite photographs of broad syndepositional syncline adjacent to steeply dipping reverse fault. For a detailed sketch of outcrop and line-length balancing and progressive restoration see Bartholomew et al. (2009, their figures 2 and 5).

B: closeup of main fault with relative displacement indicated by arrows.

C. Closeup of area around upper part of main fault showing relation of faults to an unconformity.

D. Closeup of area in the upper part of the syncline also showing relation of faults to an unconformity.

C

D

The presence of a *Ophiomorpha nodosa* burrow cutting across a small reverse fault (Bartholomew et al., 2002, their Figure 4) and the truncation of some small normal and reverse faults by minor unconformities (*Figure 19C* and *D*) while others cut across these contacts within the syncline demonstrate that the faulting occurred near the surface during deposition (Bartholomew *et al.*, 2002).

One of the main reasons for visiting this exposure is that it represents a good model for how near-surface normal and reverse faults can be related to a larger, steeply dipping reverse fault at depth. Bartholomew *et al.* (2002) used line-length balancing and restoration to remove folding and successive displacements on both the main and minor faults. We use a forward-model (*Figure 20*), derived from their restoration, to show how this structure likely evolved. As noted in the introduction, this is a likely type of structure which may be active within the modern stress field which is similar to the inferred Late Eocene stress field.

Basically, initial movement along the reverse fault a depth arches the area above the fault. Tensile stress across the arch produces strike-parallel (i.e. parallel to the main reverse fault) joints and normal faults perpendicular to S_{hmin}. If the arch has a finite length along strike then S_{hmin} and S_{Hmax} may locally switch producing cross-strike joints and normal faults along the length of the arch. Thus syndepositional orthogonal sets of joints, each with a conjugate set of normal faults, may occur in near-surface arches. Subsequently, continued displacement along the main reverse fault may rotate some normal faults to a lower angle of dip and reactivate these faults as reverse faults (Bartholomew *et al.*, 2002).

If the arch has surface expression, as was the case at Williston, then erosion may level the arch and coarse colluvial material may be deposited within the adjacent synclinal trough. In the Williston example, the colluvial material was reworked within the synclinal channel.

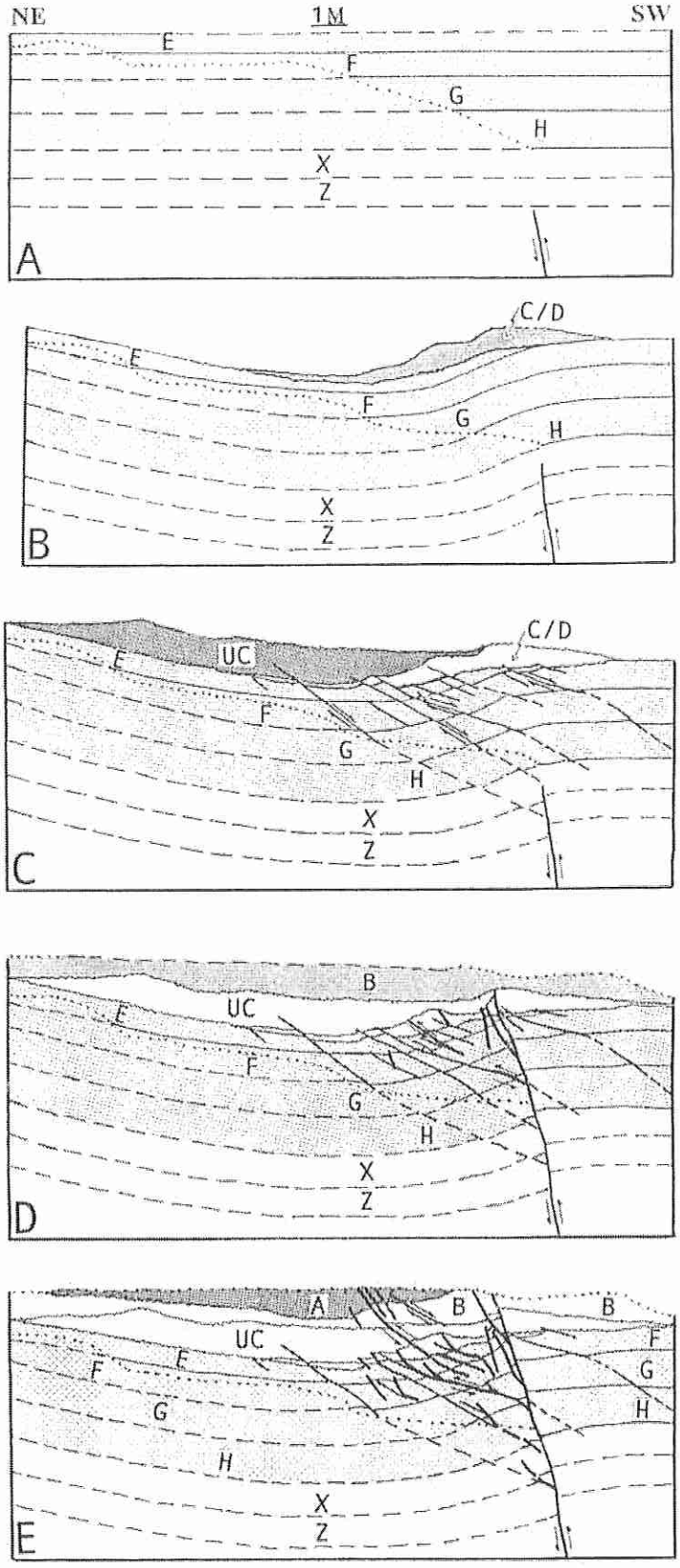

Figure 20. Sketch depicting sequential development of the growth reverse-fault and associated folds and small faults (adapted from Bartholomew et al., 2002).

A: Initial stage before growth fault has deformed beds of uniformed thickness observed in road cut. Dotted line represents base of exposed strata in road cut.

B: Reverse faulting produced near-surface fold that results in erosion of unit E from uplift and deposition of unit C/D which is partially derived from unit E.

C: Deposition of unit UC fills in trough of syncline. Tensile stress across anticlinal arch is accommodated by small, syndepositional normal faults.

D: Upward growth of main reverse fault (through units C/D and UC) causes inversion of some pre-existing normal faults into reverse faults. Deposition of unit B post-dates reverse faulting.

E: Reverse faulting again produced small near-surface fold that results in erosion of unit B and deposition of unit A which is cut by new, small, syndepositional normal faults.

Stop 6. Road cut near Bolen Mill Creek near Neeses, Orangeburg County, GA

(Figure 21)

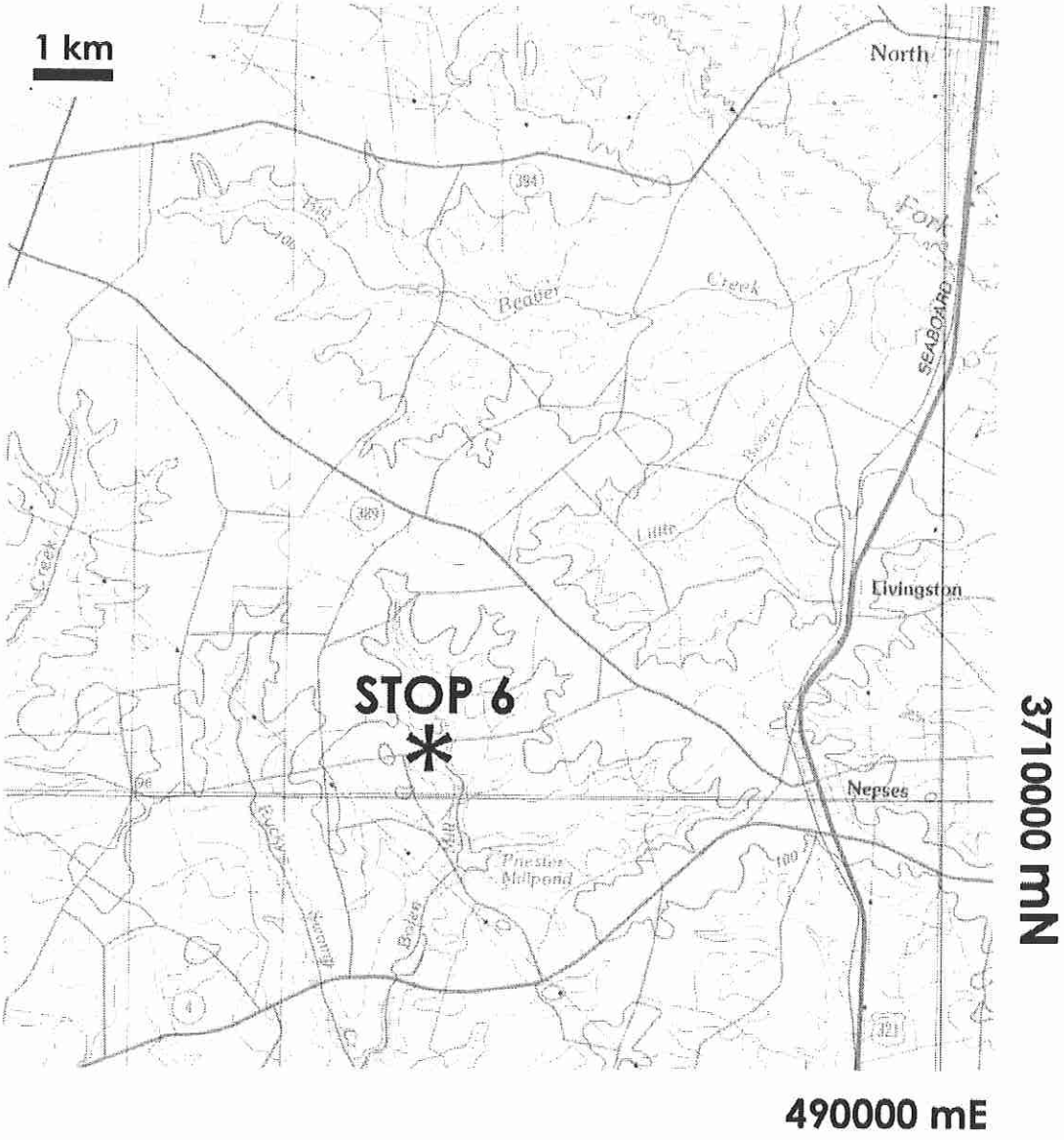

Figure 21. Map showing location of STOP 6 on a part of the Aiken, SC-GA , 1:100,000-scale quadrangle. Contour interval is 10-m.

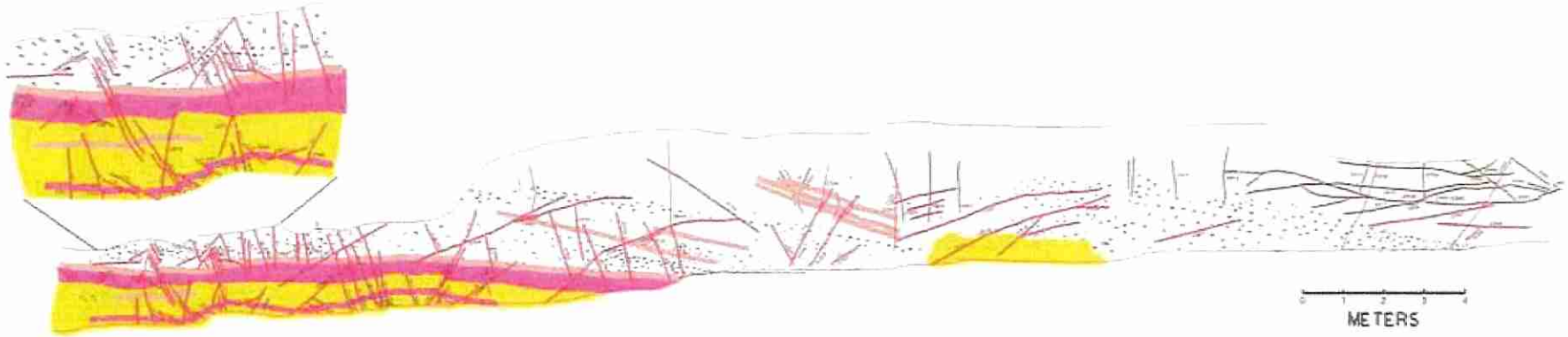

Figure 22. Sketch of road cut at SYOP 6 near Neeses, SC showing two small open folds in west end of exposure and numerous small Eocene and Miocene joints, reverse faults, and normal faults.

The structural features in this roadcut (*Figure 22*) near Neeses, SC resembles those which we have described elsewhere near Smith Lake Creek south of Martin, SC, along the railroad tracks in the southern part of the Savannah River Site, SC, and near Williston, SC (Bartholomew *et al.*, 2002) in that both Eocene and Miocene fracture sets are present. Changes in thicknesses of some units suggest that these folds (*Figure 22*) may have developed as syndepositional features, but, we have not yet done a reconstruction to see what percentage of thickness changes here are related to tectonism. Here, the smaller fold-amplitude did not result in much surface-arching and erosion like developed over the Williston structure.

Without the effects of tensile stress across a small arch, then joints only develop perpendicular to S_{hmin} rather than as orthogonal sets. Also the lack of abundant slip-vectors in these sandy beds precludes making more than just general statements about the inferred directions of S_{Hmax} and S_{hmin} for Eocene fracture sets. The three sets of inferred Eocene fractures (*Figure 23*) are consistent with the inferred counter clockwise rotation of SHmax during the late Eocene which we noted elsewhere (Bartholomew *et al.*, 2002, 2007).

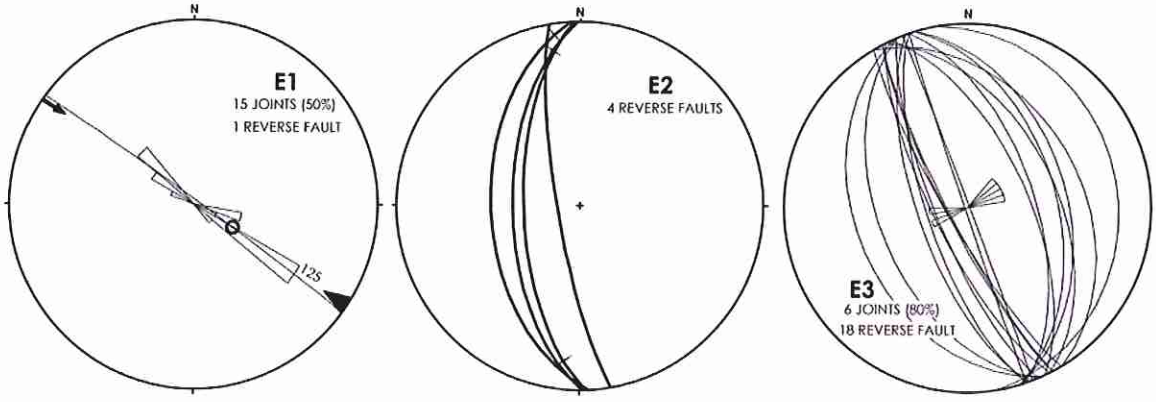

Figure 23. Eocene fracture sets at STOP 6 near Neeses, SC.
A: E1 joints and 1 reactivated reverse fault.
B: Possible E2 reactivated reverse faults.
C: E3 joints and reverse faults including joints reactivated as faults.

The four sets of inferred Miocene fractures (*Figure 24*) also are consistent with the inferred clockwise rotation of S_{Hmax} we have previously suggested. As with the Eocene fracture sets, these also have only few faults with slip-vectors, hence matching joint trends and slip-vectors is speculative here.

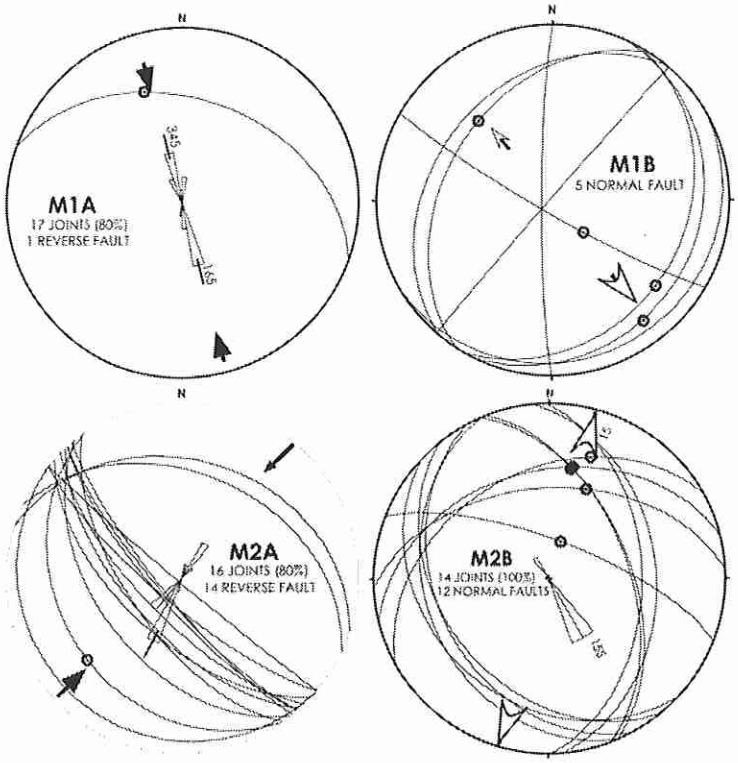

Figure 24. Miocene fracture set at STOP 6 near Neeses, SC.
A: M1A joints and 1 reverse fault.
B: Possible M1B reactivated normal faults.
C: M2A joints and reverse faults.
D: Possible M2B joints and normal faults.

Stop 7. Spillway of Lake Murray Dam, SCANA, Irmo, SC (*Figures 25* and *26*).

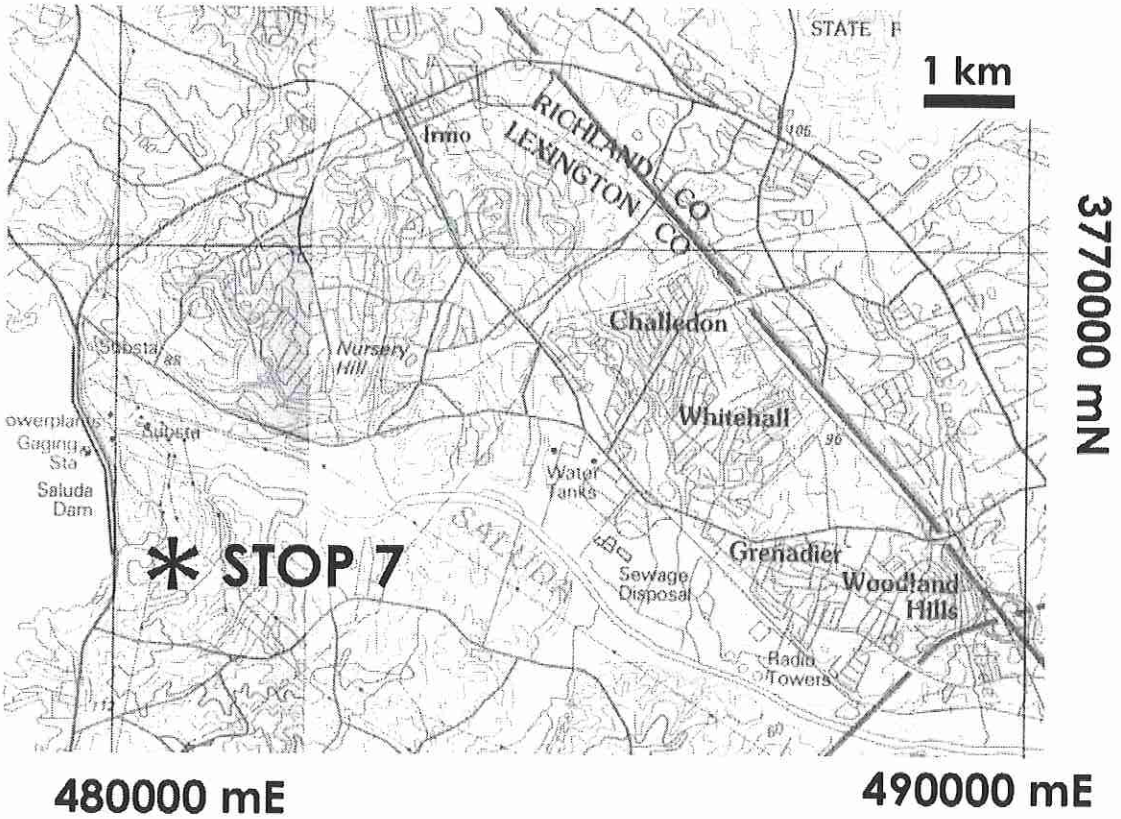

Figure 25. Map showing location of STOP 7(Figure 26) on a part of the Newberry, SC 1:100,000-scale quadrangle. Contour interval is 10-m.

In contrast to the quarries (STOP 1), the Lake Murray spillway provides an excellent place for detailed mapping of the relationships between faults, joints, and other features. Although excellent age relationships can be established from abutting and cross cutting joints and faults in the quarries, the detailed mapping in the spillway conclusively demonstrated that some joints formed as intense, en echelon arrays indicative of shearing (*Figure 27*). In particular, the set (**JR2**) related to the emplacement of the NW-trending diabase dikes is associated with shear zones. Thus these joints likely opened as Mode II joints during shearing. Also the camptonite dike (*Figure 28*) provides a good example of

how the relative age of dikes can be assessed. The dike is parallel to and contains TR3 joints. It also contains TR4, 5, and 6 joints, but does not contain TR2 joints which are found in the adjacent granitic gneiss. Thus the camptonite dike was likely emplaced during Triassic development of the J3 joint-set during the early failed rifting phase of post-Alleghanian deformation.

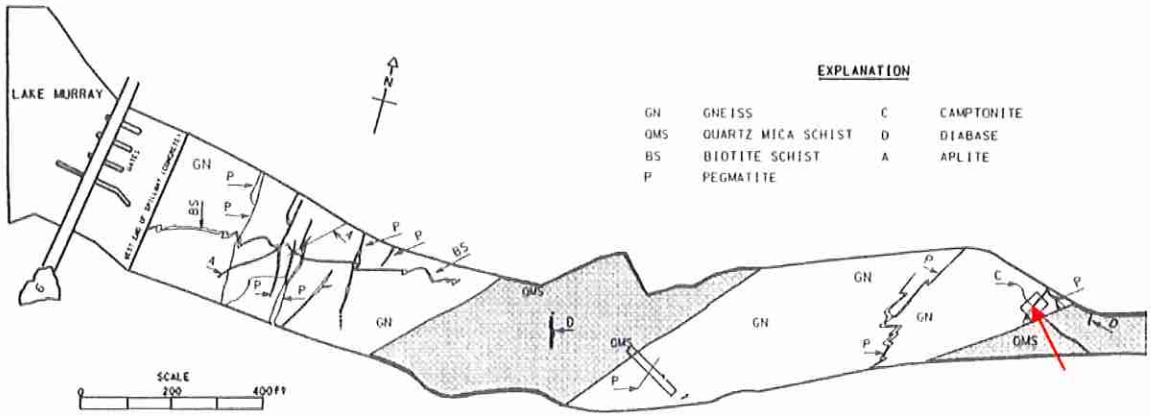

Figure 26. Generalized map of the Lake Murray Spillway from Heath, 1996). Red arrow points to map areas shown in Figures 27 and 28.

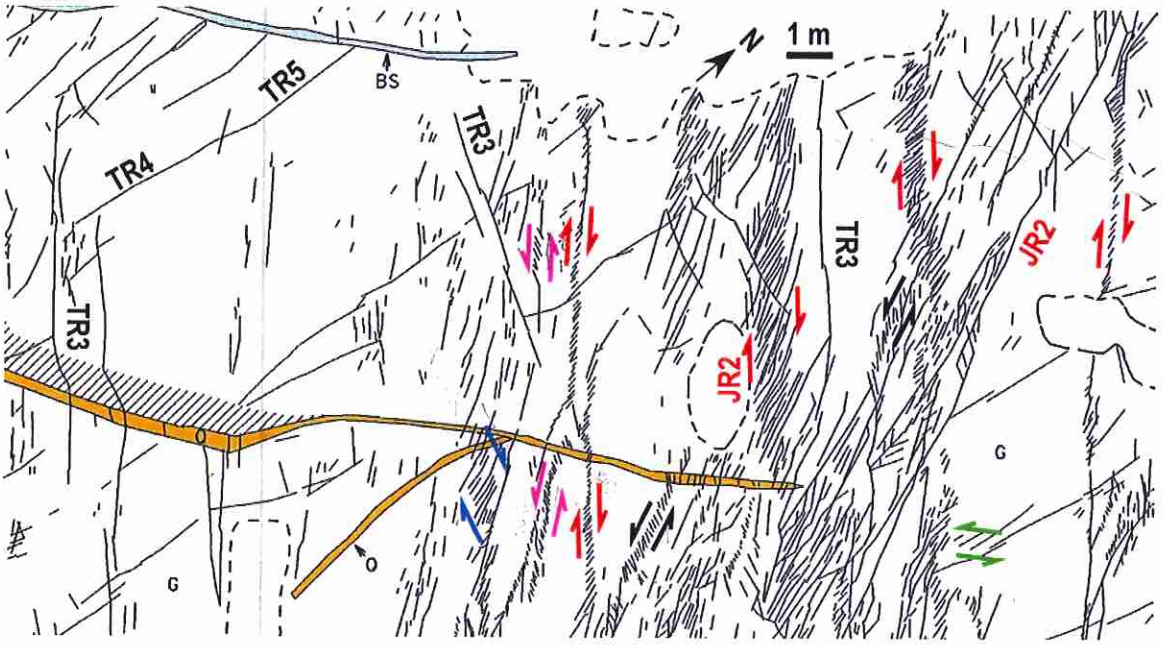

Figure 27. A map of a small area of the Lake Murray Spillway showing specific identified joints and zones of en echelon joints indicative of strike-slip shear (modified from Heath, 1996).

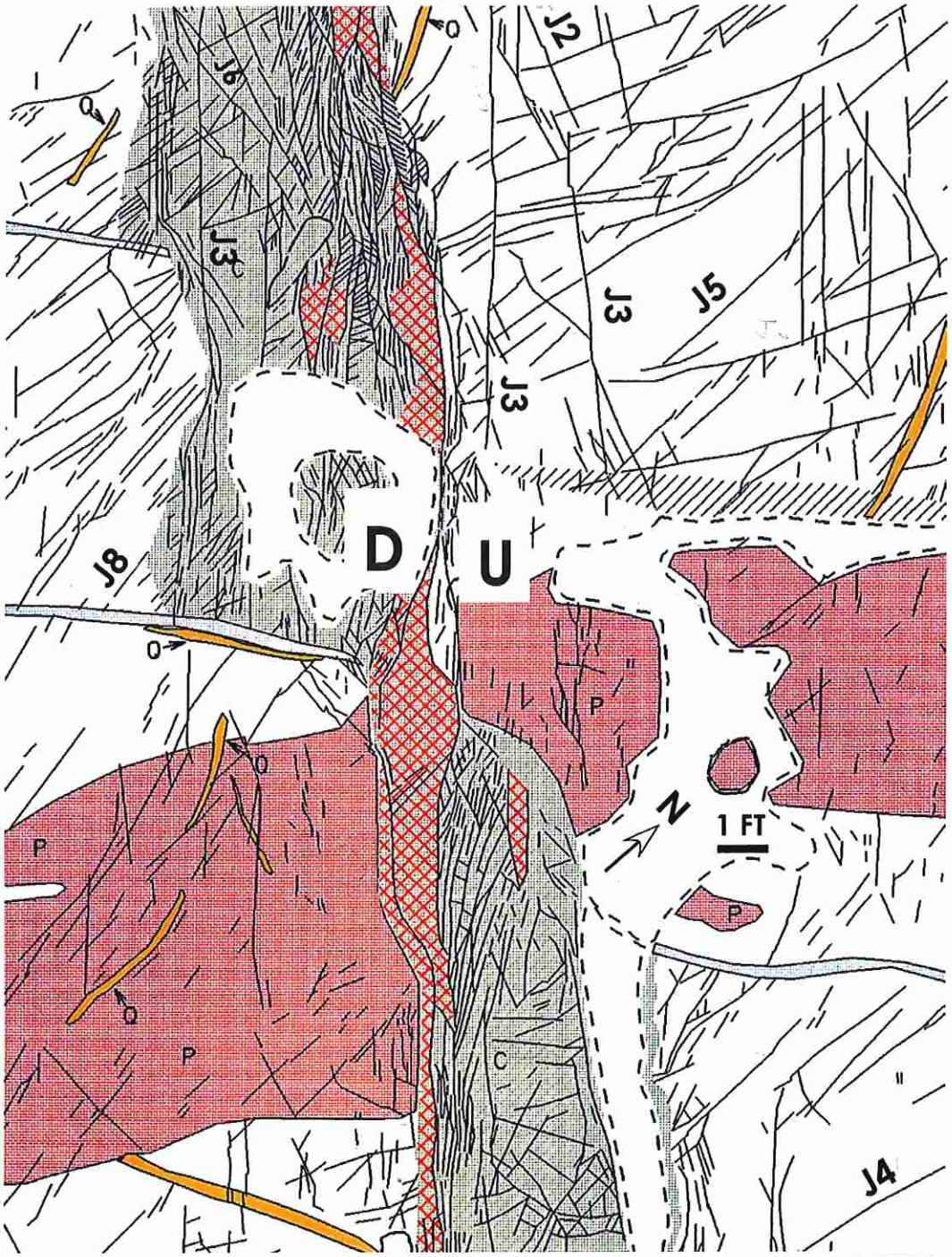

Figure 28. A map of a small area of the Lake Murray Spillway showing a camptonite dike cutting across an Alleghanian Pegmatite and subsequently cut by a subparallel fault with breccia. Representative joints are identified both within and outside of the dike (modified after Heath, 1996).

Figure 29A and B. Brecciated contact between comptonite dike and granitic gneiss in Lake Murray Spillway.

ACKNOWLEDGMENTS

This work is partially an outgrowth of the analysis of an extensive regional fracture database as part (task 169: Bartholomew) of the large project undertaken in 1994 by the South Carolina University Research and Educational Foundation (SCUREF) for the Westinghouse Savannah River Company to understand the effects of geology at the U.S. Department of Energy, Savannah River Site. We used R. W. Allmendinger's (2002) SteroWin for Windows program for doing rose diagrams and steronet plots. The 2009 field trip of the Carolina Geological Society was partially supported by Cabot Oil and Gas. We also are grateful for the cooperation of Martin Marietta Materials, Vulcan Materials Company, SCNA, and USC Aiken for their cooperation in allowing the participants on CGS 2009 to visit various sites.

REFERENCES CITED

Aadland, R. K., Gellici, J. A., and Thayer, P. A., 1995, Hydrologic framework of west-central South Carolina: State of South Carolina Department of Natural Resources, Water Resources Division Report 5, 200p.

Bakker, R. J., 2003, Package FLUIDS. Computer programs for analysis of fluid inclusion data and from modeling bulk fluid properties: Chemical Geology, v. 194, p. 3-23.

Bakker, R. J., and Brown, P. E., 2003, Computer modeling in fluid inclusion research: in Samson, I., Anderson, A., and Marshall, eds., Fluid Inclusions: Analysis and Interpretation: Mineralogical Association of Canada Short Course Series Volume 32. p. 175-212.

Bartholomew, M. J., 1998, Mesozoic and Cenozoic deformational sequence of the southern Appalachian Piedmont and Atlantic Coastal Plain: Geological Society of America, Abstracts with Program, v. 30, no. 4, p. 2.

Bartholomew, M. J., and Rich, F.J., 2001, A new method for locating possible active faults beneath the Lower Atlantic Coastal Plain, southeastern USA: Geological Society of America, Abstracts with Program, v. 33, no. 7, p. A-393.

Bartholomew, M. J., and Rich, F.J., 2002, Pleistocene shorelines and coastal rivers: sensitive indicators of Quaternary faults, Atlantic Coastal Plain, USA: EOS, Transactions, American Geophysical Union, v. 83-19, S353.

Bartholomew, M. J., and Rich, F.J., 2007, The walls of colonial Fort Dorchester: A record of structures caused the August 31, 1886 Charleston, South Carolina, earthquake and its subsequent earthquake history: Southeastern Geology, v. 44, no. 4, p. 147-169.

Bartholomew, M.J., and Whitaker, A.E., in press, The Alleghanian deformational sequence at the foreland

junction of the central and southern Appalachian, *in* Tollo, R.P., Bartholomew, M.J., Hibbard, J.P., Karabinas, P., editors, From Rodinia to Pangea: A History of the Appalachian Region: Geological Society of America Memoir.

Bartholomew, M. J., Heath, R.D., Brodie, B.M., and Lewis, S.E., 1997a, Post-Alleghanian deformation of Alleghanian granites (Appalachian Piedmont) and the Atlantic Coastal Plain: Geological Society of America, Abstracts with Program, v. 29, no. 3, p. 4.

Bartholomew, M. J., Rich, F.J., Lewis, S.E., and Brodie, B.M., 1997b, Neogene/Quaternary deformational sequence, Atlantic Coastal Plain: Geological Society of America, Abstracts with Program, v. 29, no. 6, p. A-231.

Bartholomew, M. J., Whitaker, A.E., and Barker, C.A., 1998, Preliminary Mesozoic-Cenozoic brittle-deformation history of Eocambrian rocks (Ridgeway gold mine, South Carolina), Carolina Terrane, *in* Secor, D.T., Jr., ed., Special Issue Devoted to the 1998 Field Trip of the Carolina Geological Society: South Carolina Geology, v. 40, p. 19-27.

Bartholomew, M. J., Rich F.J., Whitaker, A.E., Lewis, S.E., Brodie, B.M., and Hill, A.A., 2000, Preliminary interpretation of fracture sets in Late Pleistocene and Tertiary strata of the lower Coastal Plain in Georgia and South Carolina, *in* Abate, C., ed., Compendium of Field Trips of South Carolina Geology with Emphasis on the Charleston, South Carolina Area: South Carolina Geological Survey, Columbia, SC, p.19-27.

Bartholomew, M. J., Brodie, B.M.,Willoughby, R.H., Lewis, S.E., and Syms, F.H., 2002, Mid-Tertiary paleoseismites: Syndepositional features and section restoration used to indicate paleoseismicity, Atlantic Coastal Plain, South Carolina and Georgia, *in* Ettensohn, F.R, Rast, N., and Brett, C.E., eds., Ancient Seismites: Geological Society America, Special Paper 359: Boulder, CO, p. 63-74.

Bartholomew, M.J., Rich, F.J., Lewis, S.E., Brodie, B.M., Heath, R.D., Slack, T.Z., Trupe, C.H., III, and Greenwell, R.A., 2007, Preliminary interpretation of Mesozoic and Cenozoic fracture sets in Piedmont metamorphic rocks and in Coastal Plain strata near the Savannah River, Georgia and South Carolina, p.7-37 *in* F.J. Rich, editor, Guide to Field Trips - 56th *Annual Meeting, Southeastern Section Geological Society of America*: Georgia Southern University, Department of Geology and Geography, Contributution Series no.1, 198p.

Bodnar, R. J., 2003, Introduction to aqueous-electrolyte fluid inclusions: in Samson, I., Anderson, A., and Marshall, eds., Fluid Inclusions: Analysis and Interpretation: Mineralogical Association of Canada Short Course Series Volume 32. p. 81-100.

Bodnar, R. J., and Vityk, M. O., 1994, Interpretation of microthermometric data for H2O-NaCl fluid inclusions, in De Vivo, B., and Freezotti, M. L., eds., Fluid Inclusions in Minerals: Methods and Applications, Short Course of the Working Group (IMA) "Inclusions in Minerals", Siena, 1-4 September, 1994, p. 117-130.

Bowers, T.S., Helgeson, H.C., 1983, Calculation of the thermodynamic and geochemical consequences of nonideal mixing in the system H_2O-CO_2NaCl on phase relations in geological systems: equation of state for H_2O-CO_2-NaCl fluids at high pressures and temperatures. Geochimica et Cosmochimica Acta, v. 47, p. 1247-1275.

Boullier, A-M., 1999, Fluid Inclusions: Tectonic indicators: Journal of Structural Geology, v. 21, p. 1229-1235Bramlett, K. W., Secor, D. T., Jr., and Prowell, D. C., 1982, The Belair fault: A Cenozoic reactivation structure in the eastern Piedmont: Geological Society America Bulletin, v. 93, p.1109-1117.

Brodie, B. M., 1996, Fracture development in the upper Atlantic Coastal Plain strata, western South Carolina and eastern Georgia (M.S. Thesis): Department of Geological Sciences, University of South Carolina, Columbia, South Carolina, 56p.

Brodie, B. M., and Bartholomew, M.J., 1997, Late Cretaceous-Paleogene phase of deformation in the upper Atlantic Coastal Plain: Geological Society of America, Abstracts with Program, v. 29, no. 3, p. 7.

Colquhoun, D. J., 1965, Terrace sediment complexes in central South Carolina, *in* Atlantic Coastal Plain: Geological Association Field Conference 1965 Guidebook: Department of Geological Sciences, University of South Carolina, v. 62.

Colquhoun, D. J., 1969, Geomorphology of the lower Coastal Plain of South Carolina: South Carolina Geological Survey MS-15, 36 p.

Colquhoun, D. J., 1974, Cyclic surfical stratigraphic units of the middle and lower coastal plains, central South Carolina, *in* R. Q. Oaks and DuBar, J.R., eds., Post-Miocene Stratigraphy, Central and Southern Atlantic Coastal Plain: Utah State University Press, Logan, Utah, p. 179-190.

Colquhoun, D. J., 1981, Vairiation in sea level on the South Carolina coastal plain: UNESCO International Geological Correlation Program No. 61, The Sea Level Program, International Quaternary Association Quaternary Shoreline, Holocene and Neogene Commissions: Department of Geology, University of South Carolina, Columbia, SC, v. 181.

Colquhoun, D.J., Woollen, I.D., van Nieuwenhuise, G. G., Padgett, R. W., Oldham, D. C. Boylan, Bishop, J.W., and Howell, P.D, 1983, Surface and subsurface stratigraphy, structure, and aquifers of the South Carolina Coastal Plain (folio): University of South Carolina, Columbia, South Carolina, 78 p.

Colquhoun, D. J., Fridel, M.s., Wheeler, W.H., Daniels, R.B., Gregory, J.P., Miller, R.A., and Van Nostrand, A.K., 1987, Quaternary geologic map of the Savannah 4^{o} x 6^{o} quadrangle, United States, *in* Richmond, G.M., and Weide, D.S., eds., Miscellaneous Investigations Map I-1420, 1:100.000 scale: U. S. Geological Survey, Washington, DC.

Colquhoun, D. J., Johnson, G.G., Peebles, P.C., Huddlestun, P.F., and Scott, T., 1991, Quaternary geology of the Atlantic Coastal Plain, *in* Morrison, R.B., ed., Quaternary Nonglacial Geology: Conterminous U.S.: Geological Society of America, Geology of North America, K-2, Boulder, CO, p. 629-650.

Craw, D., 1990, Fluid evolution during uplift of the Annapurna Himal, central Nepal: Lithos, v. 24, p. 137-150.

Craw, D. and Koons, P. O., 1989, Tectonically induced hydrothermal activity and gold mineralization adjacent to major fault zones: in Keays, R., Ramsay, R., and Groves, D., eds., The Geology of Gold Deposits, Economic Geology Monograph Volume 6, p. 463-470.

Cronin, T. M., 1981, Rates and possible causes of neotectonic vertical crustal movements of the emerged southeastern United States Atlantic Coastal Plain: Geological Society of America Bulletin v. 92, p. 812-833.

Dallmeyer, R. D., Wright, J. E., Secor, D. T., Jr., and Snoke, A. W., 1986, Character of the Alleghanian orogeny in the southern Appalachians: Part II. Geochronological constraints on the tectonothermal evolution of the eastern Piedmont in South Carolina: Geological Society of America Bulletin v. 97, p.1329-1344.

Davis, L. A., and Rich, F.J., 2005, An investigation of joint sets and their relation to occurrences of rare biota at the Broxton Rocks Preserve, Altamaha Formation (Miocene), Coffee County, Georgia: Southeastern Geology, v. 44, no. 1, p. 27-36.

Diamond, L. W., 1992, Stability of CO_2 clathrate hydrate + CO_2 liquid + CO_2-vapor + aqueous KCl-NaCl solutions: Experimental determination and application to salinity estimates of fluid inclusions: Geochimica et Cosmochimica Acta, v. 56, p. 273-280.

Duan, Z., Møller, N., and Weare, J. H., 1992a, An equation of state for the CH_4-CO_2-H_2O system I. Pure

systems from 0 to 1000°C and 0 to 8000 bar: Geochemica et Cosmochemica Acta, v. 56, p. 2605-2617.

Duan, Z., Møller, N., and Weare, J. H., 1992b, An equation of state for the CH_4-CO_2-H_2O system II. Mixtures from 50 to 1000°C and 0 to 1000 bar: Geochemica et Cosmochemica Acta, v. 56, p. 2619-2631.

Dura-Gomez, I., and Talwani, P., 2009, Finding faults in the Charleston area, South Carolina: 1. Seismological data: Seismological Research Letters, v. 80, no. 5, p. 883-900.

Dutton, C. E., 1889, The Charleston earthquake of August 31, 1886: U. S. Geological Survey, Ninth Annual Report, p.203-528.

Evans, M. A. and Battles, D. A., 1999, Fluid inclusion and stable isotope analysis of veins from the central Appalachian Valley and Ridge province: Implications or regional syn-orogenic hydrologic structure and fluid migration: Geological Society of America Bulletin, v. 111, p. 1841-1860.

Evans, M. A., and Bartholomew, M. J., in press, Crustal fluid evolution and changes in deformation , uplift, and exhumation of the southeastern Piedmont of the southern Appalachians, *in* Tollo, R.P., Bartholomew, M.J., Hibbard, J.P., Karabinas, P., editors, From Rodinia to Pangea: A History of the Appalachian Region: Geological Society of America Memoir.

Evans, M. A., in press, Temporal and spatial changes in deformation conditions during the formation of the central Appalachian fold-and-thrust belt: Evidence from joints, vein mineral paragenesis, and fluid inclusions, *in* Tollo, R.P., Bartholomew, M.J., Hibbard, J.P., Karabinas, P., editors, From Rodinia to Pangea: A History of the Appalachian Region: Geological Society of America Memoir.

Fallaw, W. C., Price, V., and Sexton, W. J., 1992, Outcrops in the vicinity of the Savannah River Site, *in* Fallaw, F., and Price, V., eds., Geological Investigations of the Central Savannah River Area, South Carolina and Georgia: Carolina Geological Society Field Trip Guidebook, November 13-15, 1992: South Carolina Geological Survey, p. A-I-1-14.

Fallaw, W. C., and Price, V., 1992, Outline of stratigraphy at the Savannah River Site, *in* Fallaw, F., and Price, V., eds., Geological Investigations of the Central Savannah River Area, South Carolina and Georgia: Carolina Geological Society Field Trip Guidebook, November 13-15, 1992: South Carolina Geological Survey, p. B-II-1-33.

Garihan, J. M., and Ranson, W. A., 1992, Structure of the Mesozoic Marietta-Tryon graben, South Carolina and adjacent North Carolina, *in* Bartholomew, M. J., Hyndman, D. W., Mogk, D. W., and Mason, R., eds., Basement Tectonics 8: Characterization and Comparison of Ancient and Mesozoic Continental Margins: Kluwer Academic Publishers, Dordrecht, The Netherlands, p. 539-555.

Garihan, J. M., Preddy, M. S., and Ranson, W. A., 1993, Summary of mid-Mesozoic brittle faulting in the Inner Piedmont belt of the Carolinas, in Hatcher, R. D., Jr., and Davis, T. L., eds., Studies of Inner Piedmont Geology with a Focus on the Columbus Promontory: 1993 Carolina Geological Society Guidebook, University of Tennessee, Knoxville, TN, p.55-65.

Gillon, K. A., Mitchell, T. L., Dinkowitz, S. R., and Barnett, R. L., 1998 , The Ridgeway gold deposits: A window to the evolution of a Neoproterozoic intra-arc basin in the Carolina terrane, South Carolina, *in* Secor, D. T., Jr., ed., Special Issue Devoted to the 1998 Field Trip of the Carolina Geological Society: South Carolina Geology, v. 40, p. 1-17.

Goldstein, R. H., and Reynolds, T. J., 1994, Systematics in fluid inclusions in diagenetic minerals: SEPM Short Course 31, 199p.

Hancock, P. L., and Engelder, T., 1989, Neotectonic joints: Geological Society of America Bulletin, v. 101, p. 1197-1208.

Hatcher, R. D., Jr., Bream, B. R., and Merschat, A. J., 2007, Tectonic map of the southern and central Appalachians, *in* Hatcher, R. D., Jr., Carlson, M. P., McBride, J. H., Matinez Catalan, J. R., editors, The 4D Framework of the Continental Crust: Geological Society of America, Memoir 200, Plate 1.

Heath, R. D., and Bartholomew, M.J., 1997, Mesozoic phase of post-Alleghanian deformation in the Appalachian Piedmont: Geological Society of America Abstracts with Program, v. 29, no. 3, p. 23.

Holm, D. K., Norris, R. J., and Craw, D., 1989, Brittle and ductile deformation in a zone of rapid uplift: Central Southern Alps, New Zealand: Tectonics, v. 8, p. 153-168.

Hoyt, J. H., and Hails, J.R., 1974, Pleistocene stratigraphy of southeastern Georgia, *in* Oaks Jr., R.Q. and DuBar, J.R., eds., Post-Miocene stratigraphy, central and southern Atlantic Coastal Plain: Utah State University Press, Logan, Utah, p. 191-201.

Hoyt, J., Henry, V.J., and Weimer, R., 1968, Age of Late Pleistocene shoreline deposits, coastal Georgia, *in* Means of Correlation of Quaternary Successions, Morrison and Wright, H., eds.: University of Utah Press, Salt Lake City, UT, v. 8, p. 381-393.

Huddlestun, P. F., 1988, A revision of the lithostratigraphic units of the Coastal Plain of Georgia, the Miocene through Holocene: Georgia Geologic Survey Bulletin 104, 162 p.

Jenkin, G. R. T., Craw, D., and Fallick, A. E., 1994, Stable isotope and fluid inclusion evidence for meteoric fluid penetration into an active mountain belt; Alpine schist, New Zealand: Journal of Metamorphic Geology, v. 12, p. 429-444.

Kish, S. A., 1992, An initial geochemical and isotopic study of granite from core C-10, Savannah River Site, S.C., *in* Fallaw, F., and Price, V., eds., Geological Investigations of the Central Savannah River Area, South Carolina and Georgia: Carolina Geological Society Field Trip Guidebook, November 13-15, 1992: South Carolina Geological Survey, p. B-IV-1-7.

Madabhushi, S., and Talwani, P., 1993, Fault plane solutions and relocations of recent earthquakes in Middleton Place Summerville seismic zone near Charleston, South Carolina: Seismological Society of America Bulletin, v. 83, p. 1442-1466.

Mauldin, J., Shervais, J., and Dennis, A. J., 1997, Basement core from the Savannah River Site, South Carolina: Petrology & geochemistry of an accreted island arc: Geological Society of America Abstracts with Programs, v. 29, no. 3, p. 57.

Moos, D., and Zoback, M.D., 1993, Near-surface, "thin skin" reverse faulting stresses in the southeastern United States, *in* 34th U.S. Symposium on Rock Mechanics: International Journal of Rock Mechanics, Min. Sci. and Geomech. Abs. v. 30, p. 965-971.

Nystom, P. G., Jr., 1998, Middle Eocene to Quaternary surface stratigraphy of Girard Northwest and Shell Bluff Landing 7.5-minute quadrangles, Savannah River site, Barnwell and Aiken counties, South Carolina: South Carolina Geological Survey Open-File Report 107, 9 p. with 1:24,000-scale maps.

Nystrom, P. G., Jr., and Willoughby, R. H., 1992, Field guide to the Cretaceous and Tertiary stratigraphy of the Savannah River Site and vicinity, South Carolina: South Carolina Geological Survey, Field Guide 21, 51p.

Petit, j. p., 1987, Criteria for the sense of movementon fault surfaces in brittle rocks: Journal of Structural Geology, v. 9, p. 597-608.

Prowell, D. C., and O'Conner, B. J., 1978, Belair fault zone: Evidence of Tertiary fault displacement in eastern Georgia: Geology, v. 6, p. 681-684.

Prowell, D. C. , 1988, Cretaceous and Cenozoic tectonism on the Atlantic coastal margin, *in* Sheridan, R. E., ed., The Atlantic Continental Margin, U.S.: The Geology of North America, v. I-2: The Geological Society of America, Boulder, CO, p. 557-564.

Ragland, P. C., Hatcher, R. D., Jr., and Whittington, D., 1983, Juxtaposed diabase dike sets from the Carolinas: A preliminary assessment: Geology, v. 11, p. 394-399.

Secor, D. T., Jr., Snoke, A. W., and Dallmeyer, R. D., 1986, Character of the Alleghanian orogeny in the southern Appalachians: Part III. Regional tectonic correlations: Geological Society of America Bulletin v. 97, p.1345-1353.

Secor, D. T., Jr., Barker, C. A., Balinsky, M. G., and Colquhoun, D. J., 1998, The Carolina terrane in northeastern South Carolina: History of an exotic volcanic arc, *in* Secor, D. T., Jr., ed., Special Issue Devoted to the 1998 Field Trip of the Carolina Geological Society: South Carolina Geology, v. 40, p. 1-17.

Sibson, R. H., 1990, Rupture nucleation on unfavorably oriented faults, Bulletin of the Seismological Society of America, v. 80, p. 1580-1604.

Sutter, J. F., 1988, Innovative approaches to the dating of igneous events in the early Mesozoic basins of the eastern United States, *in* Froelich, A. J., and Robinson, G. R., Jr., eds., Proceedings, 2nd United States Geological Survey on the Early Mesozoic Basins of the Eastern United States: U. S. Geological Survey, Circular 946, p. 110-114.

Talwani, P., and Dura-Gomez, I., 2009, Finding faults in the Charleston area, South Carolina: 2. Complementary data: Seismological Research Letters, v. 80, no. 5, p. 901-919.

Weems, R. E., and Lewis, W.C., 2002, Structural and tectonic setting of the Charleston, South Carolina, region: evidence from the Tertiary stratigraphic record: Geological Society of America Bulletin 114, p. 24-42.

Willoughby, R. H., and Clendenin, C. W., 1995, Observations of faulting in an exposure along State Road 62 in Barnwell County, South Carolina: South Carolina Geological Survey Notes, no. 2, 2p.

Willoughby, R. H., Nystrom, Jr., P.G., Campbell, L.D., and Katuna, M.P., 1999, Cenozoic stratigraphic column of the Coastal Plain of South Carolina: General Geologic Chart 1, South Carolina Geological Survey, Columbia, SC.

Worrall, D.M., and Snelson, S., 1989, Evolution of the northern Gulf of Mexico, with emphasis on Cenozoic growth faulting and the role of salt, in Bally, A.W., and Palmer, A.R., editors, The Geology of North America – An overview: Boulder, Colorado, Geological Society of America, The Geology of North America, v. A, p. 97-138.

Zoback, M. D., Healy, J. H., Roller, J. C., Gohn, G. S., and Higgins, B. B., 1978, Normal faulting and in situ stress in the South Carolina coastal plain near Charleston: Geology, v. 6, p. 147-152.